



HAL
open science

Streptomyces cocklensis DSM 42063 and Actinacidiphila bryophytorum DSM 42138 colonize Arabidopsis thaliana and modulate its proteome

Florence Arsène-Ploetze, Magali Rompais, Abd El Malek Alioua, Valerie Cognat, Mathieu Erhardt, Stéfanie Graindorge, Sandrine Koechler, Jérôme Mutterer, Christine Carapito, Hubert Schaller

► To cite this version:

Florence Arsène-Ploetze, Magali Rompais, Abd El Malek Alioua, Valerie Cognat, Mathieu Erhardt, et al.. Streptomyces cocklensis DSM 42063 and Actinacidiphila bryophytorum DSM 42138 colonize Arabidopsis thaliana and modulate its proteome. *PhytoFrontiers*, 2023, 10.1094/PHYTOFR-12-22-0149-R . hal-04195921

HAL Id: hal-04195921

<https://hal.science/hal-04195921>

Submitted on 4 Sep 2023

HAL is a multi-disciplinary open access archive for the deposit and dissemination of scientific research documents, whether they are published or not. The documents may come from teaching and research institutions in France or abroad, or from public or private research centers.

L'archive ouverte pluridisciplinaire **HAL**, est destinée au dépôt et à la diffusion de documents scientifiques de niveau recherche, publiés ou non, émanant des établissements d'enseignement et de recherche français ou étrangers, des laboratoires publics ou privés.

1 ***Streptomyces cocklensis* DSM 42063 and *Actinacidiphila bryophytorum* DSM**
2 **42138 colonize *Arabidopsis thaliana* and modulate its proteome**

3

4

5 **Florence Arsène-Ploetze^{a*}, Magali Rompais^b, Abdelmalek Alioua^a, Valérie Cognat^a,**
6 **Mathieu Erhardt^a, Stefanie Graindorge^a, Sandrine Koechler^a, Jérôme Mutterer^a,**
7 **Christine Carapito^b and Hubert Schaller^a**

8

9 ^a Institut de biologie moléculaire des plantes, CNRS, Université de Strasbourg, Strasbourg,
10 France

11 ^b Laboratoire de Spectrométrie de Masse BioOrganique (LSMBO), Université de Strasbourg,
12 CNRS, IPHC UMR 7178, Infrastructure Nationale de Protéomique ProFI - FR2048 (CNRS-
13 CEA), Strasbourg, France

14

15 *** Correspondence and reprints:**

16 Florence Arsène-Ploetze

17 E-mail: florence.ploetze@ibmp-cnrs.unistra.fr

18 E-mail of the authors: rompais@unistra.fr, malek.alioua@ibmp-cnrs.unistra.fr,

19 valerie.cognat@ibmp-cnrs.unistra.fr, mathieu.erhardt@ibmp-cnrs.unistra.fr,

20 stefanie.graindorge@ibmp-cnrs.unistra.fr, sandrine.koechler@ibmp-cnrs.unistra.fr,

21 jerome.mutterer@ibmp-cnrs.unistra.fr, ccarapito@unistra.fr, [22 \[cnrs.unistra.fr\]\(http://cnrs.unistra.fr\)](mailto:hubert.schaller@ibmp-</p></div><div data-bbox=)

23 **Abstract**

24 *Streptomycetaceae* are found ubiquitously within plant microbiota. Several species belonging
25 to this family are Plant-Growth Promoting (PGP) bacteria, or may inhibit phytopathogens. Such
26 bacteria exert therefore crucial functions in host development and resistance to stresses. Recent
27 studies have shown that plants select beneficial bacteria into their microbiota. However, the
28 selection process and the molecular mechanisms by which selected bacteria modulate the
29 physiology of their host are not yet fully understood. Previous work revealed that the metabolic
30 status of *Arabidopsis thaliana* was crucial for the selection of *Streptomycetaceae* into the
31 microbiota, in particular bacteria phylogenetically related to *Streptomyces cocklensis* or
32 *Actinacidiphila bryophytorum* (previously named *Streptomyces bryophytorum*). Here, the
33 *Arabidopsis-Streptomycetaceae* interaction was further depicted by inoculating axenic *A.*
34 *thaliana* with *S. cocklensis* DSM 42063 or *A. bryophytorum* DSM 42138. We showed that these
35 two bacteria colonize *A. thaliana* ecotype Columbia-0 plants, but the colonization efficiency is
36 reduced in a *chs5* mutant of the same ecotype, bearing altered in isoprenoid, phenylpropanoid
37 and lipid profiles. We observed that *A. bryophytorum* inhibits growth of the *chs5* mutant but
38 not of the wild type, suggesting that the *Arabidopsis-Actinacidiphila* interaction depends on the
39 metabolic status of the host. Using a mass spectrometry-based proteomic approach, we showed
40 that *S. cocklensis* and *A. bryophytorum* modulate the *A. thaliana* proteome, in particular,
41 components involved in photosynthesis or phytohormone homeostasis. This study unveils
42 specific aspects of the *Arabidopsis-Streptomycetaceae* interaction and highlights its complexity
43 and diversity.

44 **Keyword:** *Streptomycetaceae*, plant metabolites, microbiota, interactions, proteome
45 **modulation**

46 1. INTRODUCTION

47 Plants host a vast array of microorganisms that collectively form a microbiota. The microbiota
48 and the host plant are considered as an ecological unit called holobiont, in which
49 microorganisms interact with their host and between them in a regulated functional network
50 (Hassani et al. 2018; Uroz et al. 2019). The microbiota fulfills functions that are important for
51 the health and development of the host and the homeostasis of the holobiont. A well-described
52 beneficial effect of certain microorganisms interacting with plants is the so-called Plant-Growth
53 Promoting (PGP) effect (Gaiero et al. 2013; Vacheron et al. 2013; Backer et al. 2018; Berg et
54 al. 2020). The mode of action of PGP Microorganisms (PGPM) is a hot research topic partly
55 because implementing PGPM in agriculture may help reduce the use of agrochemicals. PGPM
56 exert their effects through direct and indirect mechanisms. Directly, free-living or symbiotic
57 nitrogen-fixing bacteria, phosphorus-solubilizing microorganisms, hydrogen cyanide (HCN)-,
58 organic acids-, and siderophore-producing bacteria increase the availability of nutrients for the
59 plant. Indirectly, PGPM act on plant growth by producing metabolites or chemical signals that
60 modulate the host hormone balance, inhibit pathogen attacks, or promote tolerance to abiotic
61 stresses (e.g., drought, heat, or salinity). In particular, PGP bacteria (PGPB) contribute to
62 phytohormone homeostasis with the synthesis of auxin (indol acetic acid, (IAA)) and the
63 degradation of the ethylene precursor 1-AminoCyclopropane-1-Carboxylate (ACC) by the
64 enzyme ACC-deaminase, this to reduce the production of the stress hormone ethylene in the
65 host (Afzal et al. 2019). Other metabolites or signals such as polyamines, volatile organic
66 compounds (VOCs) or Acyl-Homoserine Lactones (AHL) are produced by PGPB to improve
67 stress tolerance and stimulate growth of the host. In addition, these compounds limit the
68 proliferation of pathogens and therefore produce a beneficial effect on plant fitness (Hassani et
69 al. 2018). More generally, the beneficial effect of microbiota on plant resistance to biotic or
70 abiotic stresses originates first from its ability to produce HCN, VOC, AHL, antibiotics, or cell-

71 wall degrading enzymes, secondly the negative interaction of its members with pathogens by
72 competing for nutrient or by regulating the bacterial quorum sensing-mediated responses, and
73 finally from its ability to modulate phytohormone signaling pathways and trigger the induced
74 systemic response (ISR) or the systemic acquired resistance (SAR) (Vlot et al. 2021).

75 Beneficial microorganisms interacting with host plants may be specific to one or a few
76 plant genera, species or genotypes, while others may be ubiquitously present as members of the
77 core microbiota (Schlaeppli et al. 2014; Bai et al. 2015). *Actinobacteria* are found ubiquitously
78 in plant microbiota. Among this phylum, *Streptomycetaceae* is the most abundant taxon
79 (Lundberg et al. 2012; Bulgarelli et al. 2013; Schlaeppli et al. 2014; Bai et al. 2015).
80 *Streptomycetaceae* form an important group of filamentous soil bacteria split in several genera
81 as shown by recent phylogenomic analysis (Labeda et al. 2017; Madhaiyan et al. 2022). These
82 bacteria produce mycelium allowing for their efficient colonization of the root surface or
83 internal tissues as endophytes. *Streptomycetaceae* PGPs synthesize plant growth regulators and
84 VOCs. They produce also compounds exhibiting antifungal or antibacterial activities, and
85 excrete enzymes degrading polymers such as cellulose and hemicellulose, xylan, or chitin
86 (Świecimska et al. 2022). Plant-*Streptomycetaceae* interactions have recently attracted
87 significant research efforts to elucidate the yet unknown molecular mechanisms.

88 Plants regulate the composition of their microbiota by mechanisms controlling recruitment
89 and management of beneficial microorganisms (Jones et al. 2019; Vannier et al. 2019). One of
90 this mechanisms is the plant innate immune system which affects host colonization by
91 microorganisms (Hacquard et al. 2017; Vlot et al. 2021). Another well-described mechanism
92 for the selection of microorganisms by a host plant is the production of primary and secondary
93 (also called specialized) metabolites in root exudates. These metabolites that attract beneficial
94 microorganisms and stimulate their growth, may also act as defense compounds against
95 pathogens, or act as specific signaling molecules to favor the colonization of host organs by

96 specific beneficial microorganisms. Recently, the so-called "cry-for-help" mechanism has been
97 proposed, according to which beneficial bacteria are specifically recruited when plants are faced
98 with pathogen attacks or abiotic stresses (Rizaludin et al. 2021).

99 In a previous work, we reported the effect of an impaired isoprenoid metabolism on
100 *Arabidopsis thaliana*-bacteria interactions and microbiota selection (Graindorge et al. 2022).
101 The microbiota of the wild-type genotype was compared with that of a mutant called *chs5*
102 (*chilling sensitive 5*) that had a D627N missense mutation in the enzyme 1-deoxy-D-xylulose-
103 5 phosphate synthase DXS1/CLA1/CHS5 (Schneider et al. 1995; Araki et al. 2000; Wright et
104 al. 2014). This is a limiting enzyme in the plastidial isoprenoid biosynthesis pathway (Rohmer
105 1999; Rodríguez-Concepción and Boronat 2015). This *chs5* mutant displays moderate
106 phenotypic alterations at 22°C and a chlorotic phenotype when temperature is shifted to 15°C
107 (Araki et al. 2000). In addition, untargeted metabolomic analyses revealed changes in the lipid
108 and phenylpropanoid (flavonoids, cinnamates, coumarins) profiles in addition to deficiencies
109 in carotenoids and chlorophylls (Schneider et al. 1995; Araki et al. 2000; Wright et al. 2014;
110 Graindorge et al. 2022). Interestingly, the colonization of several *Streptomycetaceae* affiliated
111 to *Actinacidiphila bryophytorum* (previously named *Streptomyces bryophytorum*) and
112 *Streptomyces cocklensis* was reduced in the *chs5* mutant regardless of growth conditions and
113 plant developmental stages. Consequently, this study (Graindorge et al. 2022) suggested that
114 the metabolic status of *A. thaliana* was crucial for the specific recruitment of *Streptomycetaceae*
115 into the microbiota.

116 The aim of the work presented here is to study the *Arabidopsis thaliana*-
117 *Streptomycetaceae* interaction *in vivo* using *A. bryophytorum* DSM 42138 and *S. cocklensis*
118 DSM42063, which are strains previously isolated from moss and soil, respectively (Kim et al.
119 2012; Li et al. 2016). To search for genes involved in plant-bacteria interaction, the genomes
120 of both bacteria were sequenced and compared. To study the effect of these two bacteria on

121 their host, we compared the proteome of inoculated and non-inoculated wild type or the *chs5*
122 plants. These data combined with growth phenotypes of inoculated seedlings and microscopic
123 observations of the bacteria *in planta* provide evidence that these bacteria specifically modulate
124 the physiology of the *A. thaliana chs5* mutant.

125 2. MATERIALS AND METHODS

126 2.1. *Arabidopsis thaliana* axenic plant growth and inoculation with *Streptomycetaceae* 127 spp.

128 *S. cocklensis* DSM 42063 and *A. bryophytorum* DSM 42138 were cultivated at 28°C on
129 a solid optimized medium for *Streptomyces* species to obtain colonies of the appropriate size
130 (>2mm) ("*Streptomyces* medium", cat. 85883, Sigma-Aldrich, Saint-Louis, Missouri, USA; the
131 composition is not given by the manufacturer). Colonies scraped with a sterile scraper were
132 resuspended in 3 ml of 10 mM MgCl₂. The suspension was centrifuged at 2500 g for 10 min
133 (repeated twice). For seed inoculation, the bacterial suspension in 10 mM MgCl₂ was adjusted
134 to 1x10⁶ to 5x10⁶ cells/ml.

135 Seeds of *A. thaliana* ecotype Colombia-0 (Col-0) and the *chs5* mutant of the same
136 genetic background were surface sterilized in 70% ethanol for 2 min, then washed in sterile
137 milliQ H₂O for 1 min. The supernatant was removed, and the seeds were treated for 5 min with
138 a commercial sodium hypochlorite solution (4%) supplemented with 0.1% Tween 20 (Sigma-
139 Aldrich, Saint-Louis, Missouri, USA). Seeds were washed 8 times with sterile milliQ H₂O then
140 air-dried. Dried seeds were placed individually with a sterile toothpick on the surface of solid
141 sterile MS medium plates (MS, 4.3 g/L Murashige & Skoog Medium M0221 (Duchefa
142 Biochemie, Haarlem, The Netherlands), 10 g/L sucrose (Euromedex, Strasbourg, France), 100
143 mg/L myo-inositol (Duchefa Biochemie, Haarlem, The Netherlands), 1 mg/L thiamine HCl
144 (Duchefa Biochemie, Haarlem, The Netherlands), 0.5 mg/L pyridoxine HCl (Duchefa
145 Biochemie, Haarlem, The Netherlands), 0.5 mg/L nicotinic acid (Duchefa Biochemie, Haarlem,
146 The Netherlands), 7 g/L agar (Sigma-Aldrich, Saint-Louis, Missouri, USA), pH 5.8). Plates
147 with seeds were kept for 2 days at 4°C in the dark before inoculation with *S. cocklensis* DSM
148 42063 or *A. bryophytorum* DSM 42138. For inoculation, each seed was covered with 5 to 7 µl

149 (5x10³ to 25x10³ cells) of bacterial suspension or sterile 10 mM MgCl₂ as negative control.
 150 Plates were then incubated in a Sanyo MLR-351 incubator (Etten-Leur, The Netherlands) under
 151 16-hour light (160 μmol photon.s⁻¹.m⁻²) at 18°C and 8-hour light (100 μmol photon.s⁻¹.m⁻²) at
 152 16°C regime. Seedlings of equivalent size (2 to 4 leaves) were transferred onto fresh MS plates
 153 after 14 days of culture. Seedlings were photographed and their phenotype was scored 24 or 31
 154 days after inoculation using Image J (segmentation based on the "Excessive Green" method
 155 described previously (Woebecke, D. M. et al. 1995)), to calculate the total leaf area and to
 156 measure the intensity of the green color of leaves.

157 2.2. Extraction and quantification of chlorophylls and carotenoids.

158 Seedlings (3 replicates of 15 seedlings each) were weighed and crushed in liquid
 159 nitrogen (with mortar and pestle). Extracts were prepared by incubating seedling materials at -
 160 20°C for 24 hours in 80% acetone (Sigma-Aldrich, Saint-Louis, Missouri, USA) in water (v/v)
 161 as previously described (Graindorge et al. 2022). Supernatants (200 μL) were transferred to 96
 162 well microplates (PS, U-bottom, MICROLON®, Greiner Bio-one, Frickenhausen, Germany).
 163 Optical density was measured for each well (in triplicate) at 470 nm, 646 nm and 663 nm on
 164 FLUOstar Omega spectrometer (BMG Labtech®, Ortenberg, Germany). The concentration of
 165 chlorophylls (C_a, C_b) and carotenoids (C_(x+c)) in samples was calculated with established
 166 formulas (Lichtenthaler and Buschmann 2001).

$$167 \quad c_a (\mu\text{g}\cdot\text{ml}^{-1}) = 12.25 A_{663} - 2.79 A_{646}$$

$$168 \quad c_b (\mu\text{g}\cdot\text{ml}^{-1}) = 21.50 A_{646} - 5.10 A_{663}$$

$$169 \quad c_{(x+c)} (\mu\text{g}\cdot\text{ml}^{-1}) = (1000 A_{470} - 1.82 c_a - 85.02 c_b)/198$$

170 c_a: concentration of chlorophyll a; c_b: concentration of chlorophyll b; c_(x+c): concentration of
 171 xanthophylls and carotenes. The concentrations of chlorophylls and carotenoids were expressed

172 in $\mu\text{g}\cdot\text{mg}^{-1}$ dry weight of plant samples.

173 **2.3. Microbiota profiling**

174 Seedlings (3 replicates of 15 seedlings each per condition) inoculated with
175 *Streptomyces* spp. or mock inoculated (24-days post inoculation) were gently removed
176 from the agar plate and crushed in liquid nitrogen (with mortar and pestle) and stored at -80°C
177 for further DNA extraction. DNA was extracted from 40 mg of frozen material using the
178 PowerPlant DNA Isolation kit (MO BIO Laboratories, Inc., Carlsbad, CA, USA). The DNA
179 concentration and quality were estimated by measuring the OD at 260 nm and 280 nm using a
180 NanoDrop™ 2000 spectrophotometer, (ThermoFischer Scientific, Waltham, MA, USA). The
181 16S rRNA-encoding gene was PCR-amplified from 12.5 ng template DNA as described
182 previously (Graindorge et al. 2022), using a mix of primers targeting the V5-V6 region (**Table**
183 **S1**). Libraries were constructed according to the 16S Metagenomic Sequencing Library
184 Preparation protocol (Illumina Part # 15044223 Rev. B,
185 [https://support.illumina.com/documents/documentation/chemistry_documentation/16s/16s-](https://support.illumina.com/documents/documentation/chemistry_documentation/16s/16s-metagenomic-library-prep-guide-15044223-b.pdf)
186 [metagenomic-library-prep-guide-15044223-b.pdf](https://support.illumina.com/documents/documentation/chemistry_documentation/16s/16s-metagenomic-library-prep-guide-15044223-b.pdf)) except some modifications as described
187 previously (Graindorge et al. 2022). After sequencing, bioinformatic processing was performed
188 using the FROGS 3.1 pipeline (Escudié et al. 2018). Briefly, it started with pre-processing of
189 the sequencing read data with “VSEARCH” (to delete PCR duplicates, too long or too short
190 reads). Then, quality sequences were clustered to operational taxonomic units (OTUs, >97%
191 sequence similarity) with “Swarm”. Chimeric OTU sequences were removed using
192 “VSEARCH”. Filtering was performed to keep OTUs present in at least 3 samples with a
193 minimal coverage of 5 sequences and suppress contaminants (phiX). Quantification were
194 performed with the Phyloseq package version 1.30.0 (sourced from Migale Bioinformatics
195 Facility, Jouy-en-Josas, France) (McMurdie and Holmes 2013).

196 2.4. Genome sequencing and mining

197 *A. bryophytorum* DSM 42138 and *S. cocklensis* DSM 42063 genomic DNAs were
198 prepared using the Wizard genomic kit (Promega, Madison, Wisconsin, USA). Genomic DNA
199 sequencing was performed *de novo* on an Illumina instrument (Illumina®, San Diego,
200 California, USA), as follows. Libraries were prepared from 100 ng genomic DNA with the
201 Nextera Flex kit (Illumina®, San Diego, California, USA). Libraries quality was assessed on
202 an Agilent Bioanalyzer (Agilent®, Agilent Technologie, Santa Clara, California, USA) using a
203 High Sensitivity DNA chip. These libraries were then loaded on a MiSeq sequencing flowcell
204 and sequenced in 2x150 paired ends mode, using a MiSeq V2 reagent kit. The 2.4×10^6 trimmed
205 reads produced an 87.5x and 102.3x coverage for DSM 42138 and DSM 42063, respectively.
206 The quality of the data was checked with FastQC version 0.11.8 (Andrews 2010). The PCR
207 duplicates were removed with fastuniq version 1.1 (Xu et al. 2012). This step excluded the
208 paired reads that were identical to keep only one. The low quality and adapters sequences were
209 trimmed with trimgalore version 0.5.0
210 (https://www.bioinformatics.babraham.ac.uk/projects/trim_galore/, based on cutadapt
211 version 1.18, (Martin 2011)). The SPAdes software was used for short read assembly (v3.13.3)
212 (Bankevich et al. 2012; Gurevich et al. 2013), with k-mers of 21, 33, 55, 77 and 99. Probable
213 contaminant scaffolds were identified (and excluded) by comparing the obtained scaffolds
214 (>500 nt) against the Microbial Genome Database (MBGD) [<http://mbgd.genome.ad.jp/>],
215 which contains 6318 genomes (2547 species, 1019 genera) including 5861 Bacteria, 254
216 Archaea and 203 Eukaryota (Last update 2018/09/20) using the megablast tool of the blast+
217 suite, version 2.9.0+.

218 A second sequencing was performed in the case of *A. bryophytorum* using the MinION
219 technology (Oxford Nanopore, Oxford, UK) to obtain a better assembly quality. Libraries were

220 prepared with 4 μ g of gDNA using the Nanopore SQKLSK109 Ligation Sequencing kit and
221 multiplexing with Nanopore EXP-NBD104 Native Barcoding Expansion kit (Oxford
222 Nanopore, Oxford, UK). Sequencing was performed with this DNA library (21.88 fmol) on a
223 Minion device with a R9.4.1 flowcell, for 48 hours as run time and realtime Guppy fast
224 basecalling. The different fastq produced by the MinKNOW software (Oxford Nanopore,
225 Oxford, UK) were fused with the Illumina reads to obtain one fastq file. A hybrid assembly by
226 combining short and long reads was performed. The data were processed with the following
227 steps to perform an assembly with high quality reads: i) PCR duplicates for Illumina paired
228 reads were removed; ii) remaining adapters from both sequencing were trimmed; iii) low
229 quality reads were trimmed ($Q < 30$ for Illumina - $Q < 10$ for Nanopore); iv) only paired end
230 reads with length >100 nt for Illumina or reads with length >1000 nt for Nanopore were
231 considered. For Nanopore reads, the quality of the data was checked with NanoPlot version
232 0.32.1 (<https://pypi.org/project/NanoPlot/>). First, the adapters were trimmed with Porechop
233 version 0.2.4 (<https://github.com/rrwick/Porechop>), then a read selection was performed with
234 FiltLong version 0.2.0 (<https://github.com/rrwick/Filtlong>, length $>1\ 000$ nt / best quality to
235 have a coverage of 100X); v) contamination and taxonomic affiliation were checked by
236 screening the library (fastq files) against standard Kraken database
237 (<https://ccb.jhu.edu/software/kraken/>) containing RefSeq genomes (archaea, bacteria, virus,
238 human, last use 14/09/2020, <https://benlangmead.github.io/aws-indexes/k2>, using the default
239 parameters), and UniVec (the NCBI vector sequence databank,
240 <https://www.ncbi.nlm.nih.gov/tools/vecscreen/univec/>) (Langmead and Salzberg 2012). The
241 completeness was evaluated using CheckM (Parks et al. 2015). The classification of the genome
242 was performed with Kraken2 version 2.0.9beta (Wood et al. 2019). Two programs were used
243 for de novo hybrid assembly: Unicycler (v0.4.8) (<https://github.com/rrwick/Unicycler>) (Wick
244 et al. 2017) and SPAdes (v3.15.2) (Bankevich et al. 2012). Different k-mer sizes to assemble

245 genomes with SPAdes (k-mers of 21, 33, 55, 77 and 99) were chosen. Unicycler is an assembly
246 pipeline for bacterial genomes, based on SPAdes. Both tools compile best contigs and scaffolds
247 for all the k-mers. The genomes analyzed for this study were integrated into the MicroScope
248 platform (<https://mage.genoscope.cns.fr/microscope/home/index.php>) and analyzed with the
249 tools available on this platform (Vallenet et al. 2006, 2009, 2013, 2017). The genomic similarity
250 was estimated with 187 *Streptomycetaceae* genomes available on the MaGe platform
251 (<https://mage.genoscope.cns.fr/microscope/> accessed on 20/08/2021), using Mash and
252 correlated to the Average Nucleotide Index (ANI) (Konstantinidis and Tiedje 2005; Ondov et
253 al. 2016). Genes previously described by several authors (Levy et al. 2017; Afzal et al. 2019;
254 Pinski et al. 2019) as genes allowing bacteria to associate with plants were searched in the
255 genome of *S. cocklensis* and *A. bryophytorum* using the "search by keywords" option of the
256 MaGe platform. We compared the metabolic capacities of these bacteria using the "Metabolic
257 Profiles" tool of the MaGe platform (Vallenet et al. 2017). The comparative genomic was
258 performed to search for genes included in the core genome using the following MICFAM
259 parameter: 80% of amino acid identity, 80% alignment coverage. The search for genes involved
260 in the synthesis of secondary metabolites was performed using the AntiSMACH prediction of
261 the MaGe platform (Blin et al. 2019). Genomic sequences were submitted to EMBL
262 (PRJEB44811 and PRJEB44812 for *S. cocklensis* and *A. bryophytorum*, respectively).

263 **2.5. Proteomic analysis**

264 *Sample preparation.* The experimental design of the proteomic analysis consisted of
265 protein extracts from wild-type and *chs5* seedlings inoculated with *S. cocklensis* DSM 42063,
266 or with *A. bryophytorum* DSM 42138, or mock inoculated, in triplicates (18 samples). Seedlings
267 (24-days post inoculation) were crushed in liquid nitrogen with a pestle in a mortar and stored
268 at -80°C for further protein extraction. Lysis buffer (1 ml: Tris 50 mM pH8, SDS 1%) was
269 added to 100 mg of frozen material in 2 ml-tubes containing 0.25-0.5 mm glass beads for

270 grinding the mixture 3 min with a Cell Disruptor Genie® (catalog number SKU: SI-DD38,
271 Scientific Industries, Bohemia, New York, USA) at 27,850 rpm. The ground mixture was
272 centrifuged at 12,000 g for 15 min at 4°C. The supernatants were transferred into new tubes
273 and protein precipitation was performed by adding 5 volumes of 0.1 M ammonium acetate in
274 100% methanol, mixing, and incubating overnight at -20°C. The pellet obtained after a 15 min
275 centrifugation step at 12,000 g was washed once with 0.1% ammonium acetate in 100%
276 methanol and dried. Unless specified, all chemicals were from Merck Sigma (Merck,
277 Darmstadt, Germany). Protein extracts were suspended in 100-130 µl of Tris 10 mM pH 6.8,
278 EDTA 1 mM, SDS 5%, glycerol 10% buffer. Protein concentration was assessed to 2-6 µg/µl
279 using a Detergent Compatible Assay (Catalog number 5000111, DC Protein Assay, Biorad,
280 Hercules, CA, USA). Reductant (10 mM DTT) and bromophenol blue (0.01%) were added to
281 the samples and 40 µg of proteins were loaded to in-house poured 5% acrylamide stacking gels.
282 Gels were stained with Coomassie Blue, and the stacking bands were manually excised.
283 Proteins were then reduced, alkylated and digested overnight at 37°C with modified trypsin in
284 a 1:100 enzyme:protein ratio (Sequencing grade Trypsin, Promega, Madison, WI, USA).
285 Peptides were extracted from the gel by gentle shaking in 80 µl of 8/2 acetonitrile/water for one
286 hour. Peptide mixtures were then dried and resuspended in 20 µl of water acidified with 0.1%
287 formic acid.

288 *Liquid Chromatography-Tandem Mass Spectrometry (LC-MS/MS) Analyses.* NanoLC-
289 MS/MS analyses of peptide extracts were performed on a NanoAcquity LC-system (Waters,
290 Milford, MA, USA) coupled to a Q-Exactive plus Orbitrap (Thermo Fisher Scientific,
291 Waltham, MA, USA) mass spectrometer equipped with a nanoelectrospray ion source. Mobile
292 phase A (99.9% water and 0.1% FA) and mobile phase B (99.9% acetonitrile and 0.1% FA)
293 were delivered at 400 nl/min. Samples were loaded into a Symmetry C18 precolumn (0.18 x 20
294 mm, 5 µm particle size, Waters) over 3 min in 1% buffer B at a flow rate of 5 µl/min. This step

295 was followed by reverse-phase separation at a flow rate of 400 nl/min using an ACQUITY
296 UPLC® BEH130 C18 separation column (250 mm x 75 µm id, 1.7 µm particle size, Waters).
297 900 ng of peptides mixtures were eluted using a gradient from 1% to 35% B in 120 min, from
298 35% B to 90% B in 1 min, maintained at 90% B for 5 min and the column was reconditioned
299 at 1% B for 20 min. The Q-Exactive plus Orbitrap instrument was operated in data dependent
300 acquisition mode by automatically switching between full MS and consecutive MS/MS
301 acquisitions. Survey full scan MS spectra (mass range 300-1800) were acquired with a
302 resolution of 70,000 at 200 m/z with an automatic gain control (AGC) fixed at 3×10^6 ions and
303 a maximum injection time set at 50 ms. The ten most intense peptide ions in each survey scan
304 with a charge state ≥ 2 were selected for MS/MS fragmentation. MS/MS scans were performed
305 at resolution 17,500 at 200 m/z with a fixed first mass at 100 m/z, AGC was fixed at 1×10^5
306 and the maximum injection time was set to 100 ms. Peptides were fragmented by higher-energy
307 collisional dissociation (HCD) with a normalized collision energy set to 27. Peaks selected for
308 fragmentation were automatically put on a dynamic exclusion list for 60 sec and peptide match
309 selection was turned on. MS data were saved in .raw file format using XCalibur software
310 3.1.66.10 (Thermo Fisher Scientific, Waltham, MA, USA).

311 *LC-MS/MS data interpretation and validation.* Raw files were converted to .mgf
312 peaklists using MSconvert and were submitted to Mascot database searches (version 2.6.2,
313 MatrixScience, London, UK) against an *A. thaliana* protein sequences database downloaded
314 from The *Arabidopsis* Information Resource TAIR site (TAIR10 gene model, 27,416 entries)
315 (Lamesch et al. 2012) concatenated with a selection of bacterial sequences downloaded on 10th
316 of July 2020 from UniprotKB (only *Streptomyces* tagged proteomes with more than 1000
317 proteins were kept, in addition to the phylogenetically related genus *Achromobacter*, total of
318 5,889,978 entries). In house assembled *S. cocklensis* and *A. bryophytorum* predicted proteomes
319 (using the illumina sequenced genomes, 17,237 entries, using the MaGe platform annotation

320 tools and process, <https://mage.genoscope.cns.fr/microscope/>) derived from the in-house
321 genome sequences (section 2.5) were also added to the database, as well as common
322 contaminants (118 entries) and decoy sequences. The concatenated target/decoy database
323 contains 2 x 5,934,749 protein entries. Spectra were searched with a mass tolerance of 5 ppm
324 in MS mode and 0.07 Da in MS/MS mode. One trypsin missed cleavage was tolerated.
325 Carbamidomethylation of cysteine residues was set as a fixed modification. Oxidation of
326 methionine residues and acetylation of proteins' N-termini were set as variable modifications.
327 Identification results were imported into Proline software (<http://proline.profi-proteomics.fr/>)
328 (Bouyssié et al. 2020) for validation. Peptide Spectrum Matches (PSM) with pretty rank equal
329 to one were retained. False Discovery Rate was then optimized to be below 1% at PSM level
330 using Mascot Adjusted E-value and below 1% at Protein Level using Mascot Mudpit score. To
331 obtain unambiguous bacterial identifications, peptide sequences shared between *A. thaliana* (or
332 contaminant proteins) and bacterial sequences were removed, as well as shared spectra (leading
333 to close but different sequences). Quantification methods and statistical analysis are presented
334 in the statistical methods section 2.7. The mass spectrometry proteomics data have been
335 deposited to the ProteomeXchange Consortium via the PRIDE (Perez-Riverol et al. 2022)
336 partner repository with the dataset identifier PXD041221 and 10.6019/PXD041221.

337 **2.6. Electron microscopy**

338 For transmission electron microscopy (TEM), leaves were incubated overnight at 4°C
339 in 3% glutaraldehyde – 3% paraformaldehyde in 0.15 M phosphate buffer at pH 7.5 for
340 fixation. Post-fixation was carried out for 2 h at room temperature in 0.5% OsO₄. After
341 staining with 0.5% Uranyl acetate, samples were dehydrated through an ethanol series from
342 50 to 100% and embedded in EPON resin (Electron Microscopy Sciences, Pennsylvania,
343 United States). Embedded leaves were sectioned with a Reichert-Jung microtome (Leica
344 Microsystems GmbH, Wetzlar, Germany) and sections were observed with a Hitachi H7500

345 TEM (Hitachi, Tokyo, Japan) at 80 kV. For scanning electron microscopy (SEM) of seeds,
346 samples were handled at a minimum to prevent bacteria dissociating from a seed. Seeds
347 underwent a graded dehydration with ethanol (70% to 100%). Final dehydration was obtained
348 in HDMS (hexamethyldisilazane). Samples were gold-palladium sputter coated and examined
349 with a Hitachi TM1000 SEM at 15 kV.

350 **2.7. Statistical methods**

351 *Analysis of chlorophylls accumulation.* The normality of the distributions and equality of
352 variances (homoscedasticity) were verified using R (version 1.4.1103) ([https://www.r-](https://www.r-project.org)
353 [project.org](https://www.r-project.org)), with a Shapiro-Wilk test and a Bartlett test, respectively, and a statistical t-test or
354 one-way ANOVA were used to analyze the chlorophylls concentrations.

355 *Microbiote profiling.* For the differential abundance of OTUs, the DEseq2 package (Love
356 et al. 2014), incremented in R was used with a Wald test to compare groups.

357 *Growth of the wild type (WT) or the chs5 mutant inoculated with A. bryophytorum DSM*
358 *42138 or S. cocklensis DSM 42063.* To compare the surface or green intensity of seedlings, the
359 normality of distributions and equality of variances (homoscedasticity) were estimated with a
360 Shapiro-Wilk test and a Bartlett test, respectively. Because at least one of both conditions were
361 not met for some samples, significant differences were evaluated using a non-parametric
362 Kruskal-Wallis test, and the *p*-value were evaluated with a Dunn test with the Bonferroni
363 correction.

364 *Proteomic analysis statistics.* For label free quantifications, peptides abundances were
365 extracted with the Proline software version 2.1 (<http://proline.profiroteomics.fr/>, (Bouyssié et
366 al. 2020)) using a *m/z* tolerance of 5 ppm. Alignment of the LC-MS runs was performed using
367 Loess smoothing and peptide identity. Cross Assignment was performed between all runs using
368 only confident features with a *m/z* tolerance of 5 ppm and a retention time tolerance of 42 sec.
369 MS-derived protein set abundances were calculated by summing the extracted ion

370 chromatogram peak intensities of all identified peptides uniquely matching to each protein set.
371 For statistical analysis, protein abundances were loaded into Prostar software version 1.22.6
372 (<http://www.prostar-proteomics.org/> (Wieczorek et al. 2017)) and associated to their
373 conditions. Proteins with 3 values in at least one condition (3 replicates) were kept for further
374 statistical analysis. Proteins identified as contaminants were removed. Protein abundances were
375 normalized using 15% quantile centering overall. Residual Missing Values were assigned in a
376 conservative way (quantile 2.5%). Pairwise Limma-tests were performed among the whole set
377 of analyses. *p*-values calibration was corrected using adapted Benjamini-Hochsberg method,
378 and FDR was optimized for each pairwise comparison. Functional annotation enrichment
379 analysis of differential proteomics data was performed in an unbiased way using the desktop
380 version of DAVID (Ease v2.0) and an updated version of gene ontology (GO) and KEGG
381 pathway databases (18th of October 2021) (Huang et al. 2009b, 2009a). The list of differential
382 proteins from each comparison of the label free experiment was compared to the list of all
383 protein matches identified. Enriched GO terms and KEGG maps were filtered by only
384 considering those with an Ease score lower than 0.1 and a Benjamini *p*-value lower than 0.05.
385 Enriched GO terms and KEGG maps were thereafter grouped together into broad functional
386 categories, which were considered as enriched broad functions.

387 3. RESULTS

388 3.1. *S. cocklensis* DSM 42063 and *A. bryophytorum* DSM 42138 genome analysis

389 Bacterial genomes were sequenced on an Illumina MiSeq sequencer. The assembly
390 yielded 156 contigs and 139 scaffolds (N50= 356,135, 8.06 Mb, with 43 scaffolds >1000nt),
391 and 232 contigs and 220 scaffolds (N50=178,610, 9.15 Mb, with 117 scaffold >1000nt) for *A.*
392 *bryophytorum* DSM 42138 and *S. cocklensis* DSM 42063, respectively. The completeness for
393 *S. cocklensis* was 99.4709 %. *A. bryophytorum* genome was also sequenced using the Nanopore
394 (MinION) technology, leading to 23 scaffold (N50=974, 8,07 Mb). The completeness for *A.*
395 *bryophytorum* was 99.4709 %. The general features of these genomes are described in **Table**
396 **S2**. The GC-contents (63.7% – 63.9%) are similar, while the size differed by 1Mb. The *S.*
397 *cocklensis* genome had more duplications (129 tandem duplications versus 113) and a higher
398 percentage of repetitive sequences compared to the *A. bryophytorum* genome (**Table S2**). The
399 genome similarity based on the Average Nucleotide Identity (ANI) was estimated with 187
400 *Streptomycetaceae* genomes. The resulting phylogram revealed that *A. bryophytorum* DSM
401 42138 was part of a clade also including *Actinacidiphila paucisporea* CGMCC 4.2025 and
402 *Actinacidiphila guanduensis* CGMCC 4.2022 (**Fig. S1**). These data support the reclassification
403 of these species into the *Actinacidiphila* genus as previously suggested (Madhaiyan et al. 2022;
404 Labeda et al. 2017). Our results revealed that *S. cocklensis* also belongs to this clade suggesting
405 that this bacterium may be included in the *Actinacidiphila* genus, but further biochemical and
406 morphological experiments are required to demonstrate this. A comparative genomic analysis
407 showed that the pan genome of the two *Streptomycetaceae* strains had 17,163 genes, while the
408 core-genome encompassed 4918 families of genes, representing 54.7%, and 61.7% of the *S.*
409 *cocklensis* and *A. bryophytorum* genes, respectively. The *S. cocklensis* and *A. bryophytorum*
410 variable genomes encompassed 45.3 and 38. 3% of the predicted ORFs, respectively, which
411 may confer specific capacities to each of these strains (**Fig. S2**).

412 3.2. Genomic features of *S. cocklensis* and *A. bryophytorum* adaptation to plants

413 We searched for genetic determinants found in plant-associated bacteria that could
414 contribute to plant colonization or plant growth promoting (PGP) capacities (Afzal et al. 2019;
415 Levy et al. 2017; Pinski et al. 2019) (**Fig. 1, Table S2**). *S. cocklensis* and *A. bryophytorum*
416 exhibited genes involved in the metabolism of fructose, D-mannose, L-arabinose, lactose,
417 ribose and xylose, which are carbohydrates found in root exudates. In *Streptomycetaceae*, γ -
418 butyrolactone (GBL) has been described as part of a Quorum Sensing (QS) system, this process
419 is known to be important for plant-bacteria interactions and for regulating antibiotic production
420 (Du et al. 2011; Polkade et al. 2016). In *S. cocklensis* genome, we identified a gene homolog to
421 *barS* (SCOCK_v1_30036) encoding an A-factor type GBL 1'-reductase, and two genes
422 (SCOCK_v1_60217 and SCOCK_v1_70112) involved in A-factor biosynthesis. These genes
423 were previously described in other bacteria as essential for the biosynthesis of GBL (Shikura et
424 al. 2002; Salehi-Najafabadi et al. 2014; Intra et al. 2016). In *A. bryophytorum*, SBRY_v2_50115
425 is also predicted to be involved in A-factor biosynthesis. Moreover, we found 29 and 27 genes
426 in *S. cocklensis* and *A. bryophytorum*, respectively, bearing more than 30% identity with GBL
427 receptors or GBL binding proteins previously characterized in other *Actinobacteria*, suggesting
428 that such signaling molecules may play a role in *S. cocklensis* and *A. bryophytorum*. Biofilm
429 formation plays an important role in the interaction between plants and bacteria (Naseem et al.
430 2018). Both bacteria have all genes required for colanic acid biosynthesis, a polysaccharide that
431 contribute to biofilm formation in *Enterobacteriaceae* and also found in one *Pseudomonas*
432 strain isolated from root endosphere (Prigent-Combaret et al. 2000; Barak et al. 2007; Zhang et
433 al. 2020). Furthermore, we found one gene in each *S. cocklensis* and *A. bryophytorum* genome
434 (SCOCK_v1_190032 and SBRY_v2_60465) displaying 49 % identity with *vbfa* from *Bacillus*
435 *subtilis*. *vbfa* encodes an acetate Na⁺-dependent symporter subunit involved in the formation
436 of biofilms under the control of volatile molecular signals (Chen et al. 2015). We identified also

437 a *bdcA* homolog (more than 43 % identity, SBRY_v2_11100, SCOCK_v1_100057 and
438 SCOCK_v1_250124) of *E. coli* that controls biofilm-related phenotypes such as cell motility,
439 cell size, cell aggregation and production of extracellular DNA and extracellular
440 polysaccharides (EPS) (Ma et al. 2011). Bacteria interacting with plant often produce cell-wall
441 degrading enzymes. We noticed that both *S. cocklensis* and *A. bryophytorum* have genes
442 required for polymer degradation, such as 1,4- β -xylan, cellulose, glycogen, and chitin.

443 We searched for PGP-related genes required for bacterial mechanisms enhancing plant
444 nutrient acquisition and growth. Both bacteria exhibited the ability to acquire phosphate through
445 four acid phosphatases (**Fig. 1, Table S2**). Both bacterial genomes also carried genes
446 homologous to *rhbACDF* involved in the synthesis of the siderophore rhizobactin produced by
447 the symbiotic nitrogen-fixing bacteria *Ensifer meliloti* (Lynch et al. 2001), and *feuV/yusV*,
448 *gobMP*, involved in iron(III)-siderophore transport. *S. cocklensis* carried *pvsABCDE* homologs
449 (SCOCK_v1_100083- SCOCK_v1_100086) required in *Vibrio alginolyticus* for iron
450 acquisition (Wang et al. 2007). Bacterial genes involved in phytohormone homeostasis were
451 found in *S. cocklensis* and *A. bryophytorum* genomes. The genes SCOCK_v1_360062 and
452 SBRY_v2_10788 had more than 30% identity with the *acdS* genes from several Gram-negative
453 symbiotic bacteria encoding the ACC-deaminase associated with plant ethylene homeostasis
454 (Tittabutr et al. 2008). *S. cocklensis* had two genes SCOCK_v1_140087 and
455 SCOCK_v1_270097 encoding an indole acetamide hydrolase and a tryptophan 2-
456 monooxygenase, respectively, required for IAA biosynthesis via the indole-3-acetamide
457 synthesis. *A. bryophytorum* had only the gene encoding a tryptophan 2-monooxygenase
458 (SBRY_v2_70106). The gene SBRY_v2_10668, SCOCK_v1_390035 shared 66.5 and 62 %
459 identity, respectively, with the "Lonely guy" (Log) gene from *Corynebacterium glutamicum*
460 ATCC 13032, acting as a cytokinin-activating protein (Seo and Kim 2017). In addition, the
461 genes SBRY_v2_11141 and SCOCK_v1_130169 shared about 36 % identity with the LOG5

462 protein from *A. thaliana* involved cytokinin biosynthesis (Kuroha et al. 2009). Other
463 phytohormone related genes were found in *A. bryophytorum* genome, like SBRY_v2_100168
464 that shared 39 % identity with the *fas5* gene of *Rhodococcus fascians* D188 strain required for
465 fasciation of its host plants (Crespi et al. 1994). SBRY_v2_100168 shared also 33 % identity
466 with the CKX4 gene of *A. thaliana* encoding a cytokinin dehydrogenase (Werner et al. 2003).
467 PGP effects may be indirectly due to the inhibition of pathogen growth by specialized
468 metabolites and antibiotics produced by beneficial microorganisms (Kim et al. 2012; van der
469 Meij et al. 2017). We identified 37 and 30 biosynthetic gene clusters (BGCs) for specialized
470 metabolites in the genome of *S. cocklensis* and *A. bryophytorum*, respectively. BGCs with high
471 completion were predicted for isorenieratene/carotenoid biosynthesis, for antibiotic or
472 antifungal compounds like griseusin, and curamycin, and for other bioactive molecules like
473 alkylresorcinol, pristinol, and 1-heptadecene, or for VOCs (geosmin, 2-methylisoborneol).
474 BGCs predicted to produce the antibacterial lipopeptide rhizomide were found in the case of *A.*
475 *bryophytorum* and BGCs predicted to produce ketomemycin were found in the case of *S.*
476 *cocklensis*.

477 Lastly, we searched for genes encoding proteins with Pfam domains enriched in plant
478 associated *Streptomyetaceae* genomes and previously predicted with five independent
479 statistical approaches (Levy et al. 2017). We searched also for plant-resembling plant-
480 associated and root-associated domains (PREPARADOs) enriched in plant-associated
481 *Streptomyetaceae* as highlighted by (Levy et al. 2017). We found most of the genes encoding
482 such proteins (18 and 17 genes in *S. cocklensis* and *A. bryophytorum*, respectively) (**Table S2**).
483 Overall, the analysis of novel genomic data generated here suggest that *S. cocklensis* and *A.*
484 *bryophytorum* have the capacity to engage various processes necessary to interact with host
485 plants. Nevertheless, 38.3 and 45.3 % of the genes of *A. bryophytorum* and *S. cocklensis*,
486 respectively, were found in only one genome (**Fig. S2**). Of these strain-specific genes, 3 (among

487 88 genes, 3.4%) and 10 (among 98 genes, 10.2%) genes from *A. bryophytorum* and *S.*
488 *cocklensis*, respectively, were proposed to be involved in plant-bacteria interactions and at least
489 16 and 20 genes (considering only complete pathways) from *A. bryophytorum* and *S. cocklensis*,
490 respectively, were proposed to be involved in secondary metabolites biosynthesis (**Table S2**).
491 These observations indicate that the metabolic, adaptive, or plant-interacting capabilities of *S.*
492 *cocklensis* and *A. bryophytorum* may be different.

493 **3.3. Exploring Plant Microbiota**

494 To find out whether bacteria affiliated to *S. cocklensis* or *A. bryophytorum* occur in the
495 microbiota of other plants, we compared the 16S rRNA sequences obtained from genomic data
496 of these two strains with those found in plant metagenomic datasets using the Joint Genome
497 Institute (JGI) BLAST tools (<https://img.jgi.doe.gov/cgi-bin/mer/main.cgi> (accessed 17 August
498 2020)). We found several sequences sharing 100% identity with the 16S rRNA sequences of *S.*
499 *cocklensis* DSM 42138 and *A. bryophytorum* DSM 42063 (with a coverage of more than 350
500 nt), in the *Arabidopsis* metagenomic datasets but also in the metagenomic data of *Populus*,
501 *Miscanthus*, Switchgrass, Corn, or Agave microbiota. Consequently, *S. cocklensis* and *A.*
502 *bryophytorum* are most probably found ubiquitously.

503 **3.4. *S. cocklensis* DSM 42063 and *A. bryophytorum* DSM 42138 colonize *A. thaliana* and** 504 **have differential effects on host growth**

505 To evaluate colonization and effects of either *Streptomycetaceae* strains on *A. thaliana*
506 growth, sterilized seeds were inoculated with *A. bryophytorum* DSM 42138 and *S. cocklensis*
507 DSM42063 and growing them under controlled conditions (**Fig. S3**). Bacterial colonization of
508 *A. thaliana* seedlings inoculated with *S. cocklensis* or *A. bryophytorum* was visualized by
509 Transmission electron microscopy (TEM) (**Fig. 2A, Fig. S4A**). Bacteria were visible on seed
510 surface as soon as four days after inoculation, although in the case of *S. cocklensis* only a few

511 bacteria were observed. *Streptomycetaceae* cells colonized also the surface of leaves after 24
512 days of seedling growth but no bacteria were detected within the leaf tissues (**Fig. 2B, Fig S4B**).
513 At the same stage, bacterial colonization of *A. thaliana* seedlings was quantified by
514 metabarcoding analysis (**Fig. 3, Fig S5**). Interestingly, the presence of bacteria affiliated to
515 *Actinobacteria*, *Proteobacteria*, *Firmicutes* *Bacteroidota* and *Acidobacteriota* was
516 demonstrated in non-inoculated seedlings even though seeds underwent a surface-sterilization
517 treatment (**Fig. S5A**). Two major OTUs named Cluster 2 and Cluster 3 detected in the
518 inoculated seedlings were affiliated to *Streptomyces* spp. and *A. bryophytorum*, respectively.
519 As expected, these OTUs were more abundant in inoculated than in non-inoculated seedlings
520 (ANOVA, p -value = 0.003 and p -value = 0.009 for Cluster 2 and Cluster 3, respectively) (**Fig.**
521 **3**), and far more abundant than other bacteria present in non-inoculated control conditions (**Fig**
522 **S5B**). Therefore, this quantitative analysis indicated that *S. cocklensis* as well as *A.*
523 *bryophytorum* colonized less efficiently the *chs5* mutant than the wild type seedlings.

524 The effect of *A. bryophytorum* and *S. cocklensis* on seedling growth was evaluated 24
525 or 31 days after inoculation (dai) by measuring their leaf surfaces (**Fig. 4**). *S. cocklensis* had a
526 small but significant growth-promoting effect on wild-type plants at 24 dai which became non-
527 significant at 31 dai. *S. cocklensis* had no significant effect on *chs5* growth at 24 or 31 dai. *A.*
528 *bryophytorum* had no significant effect on wild type seedlings at 24 or 31 dai but had a
529 significant negative effect on growth of the *chs5* mutant at 24 and 31 dai (**Fig. 4**). Overall, these
530 observations provide evidence that both bacterial species were capable of colonizing *A. thaliana*
531 wild type and the *chs5* mutant although significantly less on the latter. Both bacteria had
532 different effects on either *Arabidopsis* wild type or *chs5* mutant, and only *A. bryophytorum* had
533 a permanent negative effect on growth of the *chs5* mutant host plant.

534 **3.5. *S. cocklensis* DSM 42063 and *A. bryophytorum* DSM 42138 express proteins**
535 **involved in amino acid and carbohydrate metabolism when associated with *A.***
536 ***thaliana* in vitro**

537 To investigate the interaction between *S. cocklensis* or *A. bryophytorum* and
538 *Arabidopsis* seedlings, we carefully analyzed the proteomes of wild type or mutant holobionts,
539 to identify bacterial proteins expressed, in inoculated wild-type or mutant plants. A proper
540 differential analysis was not possible because the number of bacteria colonizing the two
541 genotypes was dramatically different (**Fig. 3**). We identified 66 proteins expressed by bacteria
542 affiliated to the *Streptomycetaceae* family. As the non-inoculated plants were still colonized by
543 few bacteria after seed sterilization (**Fig. S5**, non-inoculated plants), we focused only on 23
544 proteins, which were associated with *A. bryophytorum* or *S. cocklensis* based on genome
545 annotations and because they were detected in wild-type plants inoculated with *A.*
546 *bryophytorum* or *S. cocklensis*, but not in non-inoculated plants (**Table S3**). For 7 of these
547 proteins, at least one specific peptide was unambiguously identified as originating from *A.*
548 *bryophytorum* or *S. cocklensis* proteins in the corresponding samples inoculated with *A.*
549 *bryophytorum* or *S. cocklensis*. For the remaining 16 proteins, no specific peptide to one of
550 those two bacteria was found, i.e. we could not distinguish whether the identified protein
551 originated from *A. bryophytorum* or *S. cocklensis*. Since we inoculated with one bacterial
552 species separately, we could identify the origin of proteins ambiguously identified as part of
553 either bacteria proteome.

554 The bacterial proteins expressed *in planta* were associated with several major biological
555 processes (**Table S3**). Interestingly, *S. cocklensis* expressed an adenosylhomocysteinase
556 (SCOCK42063_v1_650034) sharing 76.1% identity with the adenosylhomocysteinase encoded
557 by the *fli* gene from *Streptantibioticus cattleyicolor* (previously named *Streptomyces cattleya*
558 (Madhaiyan et al. 2022)). This enzyme catalyzes the reversible hydrolysis of S-adenosyl-L-

559 homocysteine (AdoHcy) into homocysteine and adenosine, preventing the inhibition of the
560 fluorinase FIA required for the synthesis of fluoroacetate in this bacterium (Huang et al. 2006).
561 *A. bryophytorum* expressed a protein, SBRY_v2_40138, exhibiting 33.65% identity with a
562 perakine reductase of *Rauvolfia serpentina*, which is an aldo-keto reductase involved in the
563 biosynthesis of the monoterpene indole alkaloids such as ajmaline. *S. cocklensis* and *A.*
564 *bryophytorum* expressed two proteins involved in xylose import, suggesting a bacterial capacity
565 to use this carbohydrate when associated with plants.

566 **3.6. The *chs5* mutant is mainly impaired in its plastid/thylakoid function when grown** 567 **in axenic conditions**

568 In a next step, we compared the abundance of plant proteins in the following samples:
569 wild-type or mutant plants, inoculated or not with *S. cocklensis* or *A. bryophytorum*. A total of
570 3039 *Arabidopsis* proteins expressed in wild-type or *chs5* seedlings was found. About one tenth
571 (331 proteins) of those showed an abundance significantly different (FDR<6%) between *chs5*
572 and the wild-type, or between inoculated and non-inoculated plants (**Table S4**).

573 A differential analysis of the proteomes of non-inoculated wild-type versus *chs5*
574 seedlings (1.46% FDR, *p*-value below 0.000447) indicated that the abundance of 94 proteins
575 were significantly different between these two genotypes grown in axenic conditions (**Table**
576 **S4, columns D and E**). A functional annotation enrichment analysis of both proteomes (**Fig.**
577 **5**) revealed that 14 of the 94 proteins (14.9%) were plastid/thylakoid components or were
578 involved in RNA binding (11 were more abundant and 3 were less abundant in *chs5* than in
579 wild-type seedlings), suggesting that the *chs5* mutant is strongly impaired in its
580 plastid/thylakoid function when grown in axenic conditions. Among 15 proteins that were more
581 abundant in the wild type, we identified proteins involved in photosynthesis (2 proteins), in
582 general metabolism (2 proteins), in specialized metabolism (2 proteins), in stress response (2

583 proteins) and in plant development (1 protein) (**Table S4, columns D and E, positive**
584 **Log₂FC**). Interestingly, among these proteins, we identified a β -1,3-glucanase 3, BGLU21
585 which is a β -D-glucosidase involved in scopolin, esculin, 4-MU-glucoside or DIMBOA-
586 glucoside metabolism, and the 12-oxophytodienoate reductase 1 involved in the biosynthesis
587 of oxylipins, a class of compounds active in plant-bacteria interactions (Poloni and Schirawski
588 2014; Schenk and Schikora 2015; Stassen et al. 2021). The remaining 79 differential proteins
589 were more abundant in *chs5* than in wild-type seedlings (**Table S4, columns D and E, negative**
590 **Log₂FC**). Three proteins were enzymes involved in the plastidial isoprenoid biosynthesis: 4-
591 hydroxy-3-methylbut-2-enyl diphosphate synthase (HDS) and 4-hydroxy-3-methylbut-2-enyl
592 diphosphate reductase (HDR) acting in the isopentenylidiphosphate pathway, and
593 homogentisate prenyltransferase (PDS2) implied in the synthesis of plastoquinone-9. The other
594 proteins were involved in general metabolism, translation, protein folding and turnover, stress
595 response, plant development, hormone-mediated signaling pathway, or photosynthesis. In
596 addition, 12 ribosomal proteins were more abundant in *chs5* when compared to wild-type
597 plants. These results indicated that, under axenic and non-inoculated conditions, the *chs5*
598 mutant proteome differs from the wild-type proteome especially regarding proteins involved in
599 isoprenoid synthesis and photosynthesis, but also in plastidial translation, stress response and
600 in the synthesis of compounds that may play a role in bacteria-plant interactions.

601 **3.7. *S. cocklensis* DSM 42063 and *A. bryophytorum* DSM 42138 affect the abundance** 602 **of a common set of plant proteins**

603 To assess the impact of bacteria on the wild-type or the *chs5* proteome, we first searched
604 for proteins whose abundance was different between inoculated and non-inoculated plants. We
605 did not detect any proteins with significant differences in abundance between
606 *Streptomyces*-inoculated and non-inoculated wild-type plants. In contrast, *A.*

607 *bryophytorum*- or *S. cocklensis*-inoculated *chs5* plants displayed 24 and 23 differentially
608 abundant proteins, respectively, compared to non-inoculated *chs5* plants (**Table S4, columns**
609 **F and G, and J and K, respectively**). The abundance of 4 proteins (2 are involved in
610 photosynthesis (AT1G31330.1 (PSAF) and AT5G64040.2 (PSAN), one is involved in
611 translation, and one has an unknown function), were lower when inoculated with either *A.*
612 *bryophytorum* or *S. cocklensis*, as compared to non-inoculated *chs5*. Conversely, the abundance
613 of ELIP1 protein (AT3G22840.1) inhibiting the entire chlorophyll biosynthesis pathway, was
614 higher in inoculated as compared to non-inoculated mutant plants. These observations
615 suggested that both bacteria could modulate these same 5 proteins of the *chs5* mutant, 3 are
616 involved in photosynthesis. We observed a significant reduction of the green intensity (**Fig.**
617 **S6A**) and a reduction of chlorophylls a and b and xanthophyll and carotenoid contents in *chs5*
618 (**Fig. S6B**) inoculated with those bacteria as compared to the inoculated wild-type plants, or in
619 *chs5* inoculated with *A. bryophytorum* as compared to non-inoculated *chs5*. However, this
620 decrease was correlated with the decrease of the plant surface (**Fig. S7**). When pigments were
621 quantified per mg of dry weight, a higher amount of those pigments was observed in *chs5*
622 inoculated with *S. cocklensis*.

623 For plants inoculated with each bacterial strain, we compared the proteomes of wild
624 type vs *chs5* (**Table S4, columns H and I or L and M**). In these comparisons, we checked
625 whether plant proteins were common when inoculated with either bacterium. The abundance
626 of a common set of 81 proteins varied between wild-type or *chs5* seedlings inoculated with *A.*
627 *bryophytorum* or *S. cocklensis*, 21 of those proteins were already described as differentially
628 abundant between non-inoculated wild-type and mutant plants. The 60 other proteins are known
629 to exert functions in photosynthesis (13 proteins), general metabolism (7 proteins), translation
630 (7 proteins), protein folding or turnover (8 proteins), stress response (9 proteins) and 8 proteins
631 were related to phytohormone metabolism: ABA metabolism, perception or functions

632 (AT3G08590.1, Phosphoglycerate mutase, AT5G13630.1 magnesium-chelatase subunit *chlH*)
633 or proteins implied in biosynthesis or signaling pathways of jasmonate (AT4G22240.1 Plastid-
634 lipid associated protein PAP, AT4G04020.1 fibrillin) and auxin (AT1G06000.1 UDP-
635 Glycosyltransferase superfamily protein, AT5G64110.1 and AT1G05240.1 Peroxidase
636 superfamily protein, AT3G44300.1 nitrilase 2) (**Table S4**). These results strongly suggest that
637 both bacteria have some common effect on plant stress responses and phytohormone
638 homeostasis.

639 **3.8. *S. cocklensis* modulates the abundance of specific proteins involved in various** 640 **cellular processes in *chs5***

641 Beyond the common core proteome that vary upon colonization of both bacteria strains
642 (see below), the abundance of 18 other proteins was different in the *chs5* seedlings inoculated
643 with *S. cocklensis*, compared to the non-inoculated ones (**Table S4, columns J and K**) (5.82%
644 FDR, *p*-value below 0.000437). Inoculation of *chs5* with *S. cocklensis* led to an increase of 2
645 proteins as compared to non-inoculated seedlings: the photoreceptor PHOT1 (AT3G45780.1)
646 that regulates stomata opening and leaf photomorphogenesis, and a chloroplast thylakoid
647 protein kinase AT5G01920.1. Inoculation of *chs5* with *S. cocklensis* also led to a decrease of
648 16 proteins, four of them being related to general metabolism and among those a 1,2-alpha-L-
649 fucosidase FUC95A (AT4G34260.1) possibly acting on cell wall remodeling. Other proteins
650 are involved in oxidative stress response, translocation of proteins or lipids across chloroplasts
651 or mitochondria membranes (AT2G28900.1, AT2G38540.1, and AT5G43970.1), and one
652 protein, profilin 2 (AT4G29350.1), regulates the organization of the actin cytoskeleton.

653 Analysis of functional annotation enrichment in *chs5* plants inoculated with *S.*
654 *cocklensis* relative to wild-type inoculated plants, and in comparison with the same analysis in
655 non-inoculated plants (**Fig. 5**) suggests that *S. cocklensis* disrupts several biological processes

656 or molecular functions in wild-type or *chs5* seedlings. A comparison of the proteomes of wild-
657 type and mutant seedlings inoculated with *S. cocklensis* pointed out a variation in abundance of
658 195 proteins (0.99% FDR, *p*-value below 0.000661) (**Table S4, columns L and M**), 101 had
659 already been identified in the non-inoculated seedlings or were also differentially abundant
660 between wild-type and mutant plant inoculated with *A. bryophytorum* (**Table S4**). Among the
661 remaining 94 *S. cocklensis* specific proteins, the abundance of 58 proteins was higher in *chs5*
662 than in the wild-type plants inoculated with *S. cocklensis*. Some of these upregulated proteins
663 were related to general metabolism (9 proteins), translation or ribosome biogenesis (27
664 proteins), stress response (3 proteins), defense of plants against pathogens (3 proteins), ABA
665 homeostasis (1 proteins). The abundance of 36 specific proteins was higher in the inoculated
666 wild-type than in *chs5* plants. These proteins had functions in photosynthesis (11 proteins),
667 general metabolism (7 proteins), stress response (2 proteins), and defense of plants against
668 pathogens (5 proteins) (**Table S4**).

669 **3.9. In the presence of *A. bryophytorum*, the abundance of specific proteins involved in**
670 **the ABA-mediated stress response was altered in the *chs5* mutant.**

671 Beyond the common core of proteins that vary upon colonization of both bacteria strains
672 (see below), the abundance of 19 specific proteins (4.55% FDR, *p*-value below 0.000363) was
673 different in the *chs5* seedlings inoculated with *A. bryophytorum*, compared to the non-
674 inoculated ones (**Table S4, columns F and G**). Seedlings of the *chs5* mutant exhibited an
675 increase in the abundance of 8 proteins when inoculated with *A. bryophytorum*. Among those,
676 Fibrillarlin 2, a negative regulator of the expression of immune responsive genes,
677 AT1G13930.1, a protein categorized as salt stress responsive, and AT1G06000.1 an UDP-
678 Glycosyltransferase acting in flavonol biosynthesis. Seedlings of the *chs5* mutant inoculated
679 with *A. bryophytorum* exhibited also a decrease of the abundance of 11 proteins, among which
680 the oxylipin biosynthetic enzyme allene oxide synthase CYP74A (AT5G42650.1), two proteins

681 probably associated with the light/cold stress-related jasmonate (JA) biosynthesis
682 (AT1G77490.1 and AT2G35490.1), and PCAP1 (plasma-membrane associated cation-binding
683 protein, AT4G20260.4) and PATL1 (AT3G14210.1) and PATL2 (AT1G22530.1), which are
684 phosphoinositide interacting proteins involved in membrane-trafficking events associated with
685 cell plate formation during cytokinesis.

686 Analysis of functional annotation enrichment in *chs5* plants inoculated with *A.*
687 *bryophytorum* relative to wild-type inoculated plants, and in comparison with the same analysis
688 in non-inoculated plants, suggests that this bacterium modulates the abundance of abiotic stress-
689 related proteins (**Fig. 5**). A comparison of the proteomes of wild-type and mutant plants
690 inoculated with *A. bryophytorum* revealed that the abundance of 157 proteins varied (0.98%
691 FDR, *p*-value below 0.000525) (**Table S4, columns H and I**), among which 90 had already
692 been discussed previously when comparing non-inoculated wild-type and mutant seedlings or
693 were identified as differentially abundant in wild type vs mutant plant inoculated with *S.*
694 *cocklensis* (see previous paragraphs). Among the remaining 67 *A. bryophytorum* specific
695 proteins), the abundance of 20 proteins was higher in *chs5* than in the wild type when inoculated
696 with *A. bryophytorum*, especially proteins involved in general metabolism (4 proteins), in
697 translation or ribosome biogenesis (3 proteins), stress response (2 proteins) and ABA
698 homeostasis (1 proteins) (**Table S4**). A set of 47 proteins was specifically more abundant in the
699 wild-type than in mutant plants, some of which being involved in photosynthesis (18 proteins),
700 general metabolism (3 proteins), stress response (6 proteins) and auxin, ABA and jasmonate
701 homeostasis (3 proteins). These results suggest that in the presence of *A. bryophytorum*, *chs5*
702 seedlings exhibit different metabolism, photosynthesis capacities, and responses to stress, in
703 particular those related to ABA, jasmonate and auxin, as compared to the wild type.

704 In conclusion, it appears that proteomes from *chs5* seedlings colonized by *S. cocklensis*
705 or *A. bryophytorum* are broadly modified when compared to the proteome of axenic *chs5*

706 seedlings. Overall, the differences between wild-type and mutant proteomes of inoculated
707 seedlings are proteins of a wide range of functions, even more so than in non-inoculated
708 seedlings. Both bacteria apparently affect the abundance of a common set of proteins known to
709 play a role in photosynthesis. Nevertheless, in addition to this common set, these two bacteria
710 modify the abundance of different *Arabidopsis* proteins associated with various cellular
711 processes like phytohormone homeostasis or stress responses. Such a change in the proteome
712 profiles of *chs5* is most likely responsible, at least in part, for its reduced growth, particularly
713 in the presence of *A. bryophytorum* (Fig. 4).

714 4. DISCUSSION

715 Plant organs and tissues are the hosts of microbial communities (or microbiota) that
716 consequently form holobiont entities. Our previous work revealed that the metabolic status of
717 *A. thaliana* was crucial for the colonization of *Streptomycetaceae* into the microbiota, in
718 particular, those affiliated to *A. bryophytorum* and *S. cocklensis* (Graindorge et al. 2022). The
719 aim of this work was to study the interaction between wild-type or mutant *A. thaliana* and *A.*
720 *bryophytorum* DSM 42138 and *S. cocklensis* DSM 42063, isolated from moss and soil,
721 respectively (Kim et al. 2012; Li et al. 2016). We indeed confirmed that these two bacteria
722 colonize *A. thaliana*. The results presented here demonstrate a decreased colonization of *A.*
723 *bryophytorum* and *S. cocklensis* in the *chs5* mutant that carries a weak allele of the gene coding
724 for DXS1, a key enzyme of the plastidial MEP pathway, as compared to the wild type. This is
725 in full accordance with our previous observations suggesting that colonization and/or growth
726 of *A. bryophytorum* or *S. cocklensis* are reduced when these bacteria interact with this *chs5*
727 mutant (Graindorge et al. 2022). Since the *chs5* mutant has defects in the synthesis of
728 isoprenoids, phenylpropanoids and lipids, these metabolites could participate in the recruitment
729 of *A. bryophytorum* and *S. cocklensis* by the wild-type plant, and /or colonization or bacterial
730 growth when associated to the host plant. In this study, in addition to metabolites, we observed

731 significant variations in the *chs5* proteome, compared to the wild type. The detailed proteome
732 analysis of the *chs5* mutant confirms a major deficit of the plastid/thylakoid function.
733 Interestingly, we also observed variation in the abundance of proteins related to stress
734 responses, photosynthesis and hormone homeostasis or perception. We cannot exclude that
735 those variations may directly or indirectly affect bacterial colonization.

736 This study enabled us to study the mechanisms of interactions between
737 *Streptomycetaceae* and *Arabidopsis*. When associated with their host, *A. bryophytorum* and *S.*
738 *cocklensis* expressed proteins involved in xylose import and a glyceraldehyde-3-phosphate
739 dehydrogenase, suggesting that xylose can be used by the bacteria and further transformed via
740 the glycolysis pathway. Interestingly, xylose is one of the most important carbohydrate
741 produced in *Arabidopsis* roots (Peng et al. 2000). Other proteins expressed by the bacteria may
742 be important for their interaction with their host. For example, *S. cocklensis* expressed an
743 adenosylhomocysteinase and *A. bryophytorum* expressed a protein, SBRY_v2_40138, which is
744 an aldo-keto reductase involved in the biosynthesis of monoterpenoid indole alkaloids.
745 Interestingly, proteins containing an aldo-keto reductase domain (Pfam00248) were enriched
746 in the genome of plant-associated bacteria, suggesting that metabolites generated by such
747 enzymatic activity may be important for plant-bacteria interactions (Levy et al. 2017). These
748 proteomic data suggest that a metabolic interaction is possible between *A. thaliana* and *A.*
749 *bryophytorum* or *S. cocklensis*.

750 *Streptomycetaceae* have the capacities to promote growth of plants (PGP) (Olanrewaju
751 and Babalola 2019). We observed that *S. cocklensis* had a temporary minor but significant PGP
752 effect on wild-type *Arabidopsis thaliana* using the seedling growth bioassay described in this
753 work. This bacterium exhibit genes for the synthesis of IAA, which may be responsible for this
754 PGP effect, as previously observed with other *Streptomycetaceae* (Fu et al. 2022). This minor
755 PGP effect was not observed when the *chs5* mutant seedlings were inoculated with *S.*

756 *cocklensis*, and a negative effect on growth was visible in the case of *chs5* inoculated with *A.*
757 *bryophytorum*. These observations suggest that the *chs5* seedlings, but not the wild-type
758 seedlings, have several defects and must withstand adverse conditions when inoculated with *A.*
759 *bryophytorum*. Thus, the interaction between *Arabidopsis* and these two *Streptomycetaceae*
760 could be defined as neutral in a wild-type context but, in the case of *A. bryophytorum*, harmful
761 in the *chs5* background where isoprenoid, phenylpropanoid and lipid syntheses are partially
762 impaired.

763 Both bacteria modulate the plant *chs5* proteome, revealing that colonization by these
764 bacteria influences plant physiology. *A. bryophytorum* and *S. cocklensis* share a common effect
765 on plant stress responses and phytohormone homeostasis. However, each bacterium also has
766 specific effects on the *Arabidopsis* proteome, as shown in **Figure 5**. The abundance of proteins
767 involved in general metabolism was different between the wild-type and the *chs5* seedlings
768 inoculated with *S. cocklensis* DSM 42063, whereas the abundance of proteins implied in the
769 response to abiotic stresses was different between the wild-type and in *chs5* seedlings
770 inoculated with *A. bryophytorum* DSM 42138. These variations could be at least partly
771 responsible for the reduced growth of *chs5* in the presence of *A. bryophytorum*. Inoculation of
772 *chs5* with this strain led to an increase of the fibrillarlin 2 that acts as a negative regulator of the
773 expression of immune responsive genes, and of a protein involved in the regulation of abscisic
774 acid (ABA) biosynthesis (AT1G13930.1). This observation indicates that *A. bryophytorum* may
775 directly or indirectly manipulate the immune response of its mutated host or modulate ABA
776 homeostasis. This effect on plant immune response or ABA homeostasis may indirectly play a
777 role in the abiotic stress response (drought or salinity for example) and/or change the capacity
778 of the plant to resist to pathogens. *A. bryophytorum* may therefore modulate the induced
779 systemic response (ISR) (Pinski et al. 2019; Vlot et al. 2021). Remarkably, *chs5* plants were
780 less efficiently colonized by bacteria affiliated to *Streptomycetaceae* and were more sensitive

781 to *Pseudomonas syringae* infection when grown in holoxenic conditions (Graindorge et al.
782 2022). The *Streptomyetacea*-dependent tuning of the *Arabidopsis* immune response observed
783 in this study under gnotoxenic conditions could be in part responsible for the increased
784 pathogen susceptibility of the *chs5* mutant observed previously under holoxenic conditions
785 (Graindorge et al. 2022). However, further studies are needed to characterize a possible
786 modulation of the immune response induced by *A. bryophytorum*. In addition, other indirect
787 effect could be proposed to explain the above observations. For example, these bacteria have
788 the capacity to produce antibiotics, which is crucial for the biocontrol effect previously
789 described for such bacteria (van der Meij et al. 2017; Olanrewaju and Babalola 2019). *S.*
790 *cocklensis* produces the antibiotic dioxamycin (Kim et al. 2012). *S. cocklensis* and *A.*
791 *bryophytorum* probably produce other antibiotics, since we found in their genomes more than
792 30 clusters of genes with a putative role in the synthesis of antibiotic and specialized
793 metabolites.

794 Our data revealed that each bacterial strain had distinct effect on their host and the
795 genomic content of *A. bryophytorum* and *S. cocklensis* was different in terms of gene content,
796 for example genes involved in plant-bacteria interactions. *A. bryophytorum* and *S. cocklensis*
797 are two phylogenetically closely related strains but the genomic data indicate that the variable
798 genome otherwise known as dispensable genome of these two *Streptomyetaceae* strains
799 encompass 45.3 and 38.3% of the predicted ORFs. In fact, genomes of *Streptomyetaceae*
800 strains are indeed quite divergent with large dispensable regions localized in the sub-telomeric
801 part of their linear genome (Kim et al. 2015; Bu et al. 2020).

802 Finally, the results presented here are consistent with a specific selection of
803 *Streptomyetaceae* by *Arabidopsis* via signals or perception mechanisms involving isoprenoids,
804 phenylpropanoids and/or lipids. Database searches suggest that bacteria affiliated to *S.*
805 *cocklensis* or *A. bryophytorum* are found in the microbiota of other plants. It is therefore most

806 likely that the bacterial effect observed here in the case of *Arabidopsis* could also be observed
807 with other plants. Overall, the work presented here provides a better understanding of the
808 molecular mechanisms involved in the interaction between *Streptomyetaceae* and *A. thaliana*
809 and, more broadly, the selection mechanisms of the plant microbiota.

810 5. CONFLICT OF INTEREST:

811 The authors declare no conflict of interest.

812 6. ACKNOWLEDGEMENTS

813 H.S. warmly thanks Toshiya Muranaka and Koh Iba for a gift of *Arabidopsis thaliana chs5*
814 seeds. This work was supported by the Université de Strasbourg (UdS) and the Centre National
815 de la Recherche Scientifique (CNRS). The LABGeM (CEA/Genoscope & CNRS UMR8030),
816 the France Génomique and French Bioinformatics Institute national infrastructures (funded as
817 part of Investissement d'Avenir program managed by Agence Nationale pour la Recherche,
818 contracts ANR-10-INBS-09 and ANR-11-INBS-0013) are acknowledged for support within
819 the MicroScope annotation platform. The French Proteomic Infrastructure (ProFI; ANR-10-
820 INBS-08-03, FR2048) is acknowledged for its support in the MS-based proteomics analysis.

821 7. AUTHOR CONTRIBUTIONS

822 M.R., S.G, S.K., C.C., H.S. and F.A.-P. conceived, planned, and designed the research. F.A-P.
823 performed extraction and quantification of chlorophylls and carotenoids. S.G., S.K. and F.A-P
824 performed microbiota profiling. S.K. A.A. and V.C. sequenced and assembled the bacterial
825 genomes. M.R. and C.C conducted MS-proteomics experiments and data analysis. J.M.
826 quantified the rosette surface and green intensity using Image J. M.E. performed electron
827 microscopy. F.A.-P. performed *in vitro* experiments and analyzed proteomic and genomic data.
828 H.S. and F.A.-P. wrote the manuscript.

829 8. REFERENCES

830 Afzal, I., Shinwari, Z. K., Sikandar, S., and Shahzad, S. 2019. Plant beneficial endophytic
831 bacteria: Mechanisms, diversity, host range and genetic determinants. Microbiol. Res.
832 221:36–49.

- 833 Andrews, S. 2010. FastQC: a quality control tool for high throughput sequence data.
- 834 Araki, N., Kusumi, K., Masamoto, K., Niwa, Y., and Iba, K. 2000. Temperature-sensitive
835 Arabidopsis mutant defective in 1-deoxy-d-xylulose 5-phosphate synthase within the plastid
836 non-mevalonate pathway of isoprenoid biosynthesis. *Physiol. Plant.* 108:19–24.
- 837 Backer, R., Rokem, J. S., Ilangumaran, G., Lamont, J., Praslickova, D., Ricci, E., et al. 2018. Plant
838 Growth-Promoting Rhizobacteria: context, mechanisms of action, and roadmap to
839 commercialization of biostimulants for sustainable agriculture. *Front. Plant Sci.* 9.
- 840 Bai, Y., Müller, D. B., Srinivas, G., Garrido-Oter, R., Potthoff, E., Rott, M., et al. 2015. Functional
841 overlap of the Arabidopsis leaf and root microbiota. *Nature.* 528:364–369.
- 842 Bankevich, A., Nurk, S., Antipov, D., Gurevich, A. A., Dvorkin, M., Kulikov, A. S., et al. 2012.
843 SPAdes: a new genome assembly algorithm and its applications to single-cell sequencing. *J.*
844 *Comput. Biol. J. Comput. Mol. Cell Biol.* 19:455–477.
- 845 Barak, J. D., Jahn, C. E., Gibson, D. L., and Charkowski, A. O. 2007. The role of cellulose and O-
846 antigen capsule in the colonization of plants by *Salmonella enterica*. *Mol. Plant-Microbe*
847 *Interact. MPMI.* 20:1083–1091.
- 848 Berg, G., Rybakova, D., Fischer, D., Cernava, T., Vergès, M.-C. C., Charles, T., et al. 2020.
849 Microbiome definition re-visited: old concepts and new challenges. *Microbiome.* 8:103.
- 850 Blin, K., Shaw, S., Steinke, K., Villebro, R., Ziemert, N., Lee, S. Y., et al. 2019. antiSMASH 5.0:
851 updates to the secondary metabolite genome mining pipeline. *Nucleic Acids Res.* 47:W81–
852 W87.
- 853 Bouyssié, D., Hesse, A.-M., Mouton-Barbosa, E., Rompais, M., Macron, C., Carapito, C., et al.
854 2020. Proline: an efficient and user-friendly software suite for large-scale proteomics.
855 *Bioinforma. Oxf. Engl.* 36:3148–3155.

- 856 Bu, Q.-T., Li, Y.-P., Xie, H., Wang, J., Li, Z.-Y., Chen, X.-A., et al. 2020. Comprehensive dissection
857 of dispensable genomic regions in *Streptomyces* based on comparative analysis approach.
858 *Microb. Cell Factories*. 19:99.
- 859 Bulgarelli, D., Schlaeppli, K., Spaepen, S., Ver Loren van Themaat, E., and Schulze-Lefert, P.
860 2013. Structure and functions of the bacterial microbiota of plants. *Annu. Rev. Plant Biol.*
861 64:807–838.
- 862 Chen, Y., Gozzi, K., and Chai, Y. 2015. A bacterial volatile signal for biofilm formation. *Microb.*
863 *Cell*. 2:406–408.
- 864 Crespi, M., Vereecke, D., Temmerman, W., Van Montagu, M., and Desomer, J. 1994. The *fas*
865 operon of *Rhodococcus fascians* encodes new genes required for efficient fasciation of host
866 plants. *J. Bacteriol.* 176:2492–2501.
- 867 Du, Y.-L., Shen, X.-L., Yu, P., Bai, L.-Q., and Li, Y.-Q. 2011. Gamma-butyrolactone regulatory
868 system of *Streptomyces chattanoogensis* links nutrient utilization, metabolism, and
869 development. *Appl. Environ. Microbiol.* 77:8415–8426.
- 870 Escudié, F., Auer, L., Bernard, M., Mariadassou, M., Cauquil, L., Vidal, K., et al. 2018. FROGS:
871 Find, Rapidly, OTUs with Galaxy Solution. *Bioinforma. Oxf. Engl.* 34:1287–1294.
- 872 Fu, W., Pan, Y., Shi, Y., Chen, J., Gong, D., Li, Y., et al. 2022. Root morphogenesis of *Arabidopsis*
873 *thaliana* tuned by plant growth-promoting *Streptomyces* isolated from root-associated soil of
874 *Artemisia annua*. *Front. Plant Sci.* 12.
- 875 Gaiero, J. R., McCall, C. A., Thompson, K. A., Day, N. J., Best, A. S., and Dunfield, K. E. 2013.
876 Inside the root microbiome: bacterial root endophytes and plant growth promotion. *Am. J.*
877 *Bot.* 100:1738–1750.

- 878 Graindorge, S., Villette, C., Koechler, S., Groh, C., Comtet-Marre, S., Mercier, P., et al. 2022.
879 The *Arabidopsis thaliana*–*Streptomyces* interaction is controlled by the metabolic status of
880 the holobiont. *Int. J. Mol. Sci.* 23:12952.
- 881 Gurevich, A., Saveliev, V., Vyahhi, N., and Tesler, G. 2013. QUASt: quality assessment tool for
882 genome assemblies. *Bioinforma. Oxf. Engl.* 29:1072–1075.
- 883 Hacquard, S., Spaepen, S., Garrido-Oter, R., and Schulze-Lefert, P. 2017. Interplay between
884 innate immunity and the plant microbiota. *Annu. Rev. Phytopathol.* 55:565–589.
- 885 Hassani, M. A., Durán, P., and Hacquard, S. 2018. Microbial interactions within the plant
886 holobiont. *Microbiome.* 6:58.
- 887 Huang, D. W., Sherman, B. T., and Lempicki, R. A. 2009a. Bioinformatics enrichment tools:
888 paths toward the comprehensive functional analysis of large gene lists. *Nucleic Acids Res.*
889 37:1–13.
- 890 Huang, D. W., Sherman, B. T., and Lempicki, R. A. 2009b. Systematic and integrative analysis
891 of large gene lists using DAVID bioinformatics resources. *Nat. Protoc.* 4:44–57.
- 892 Huang, F., Haydock, S. F., Spiteller, D., Mironenko, T., Li, T.-L., O’Hagan, D., et al. 2006. The
893 gene cluster for fluorometabolite biosynthesis in *Streptomyces cattleya*: a thioesterase
894 confers resistance to fluoroacetyl-coenzyme A. *Chem. Biol.* 13:475–484.
- 895 Intra, B., Euanorasetr, J., Nihira, T., and Panbangred, W. 2016. Characterization of a gamma-
896 butyrolactone synthetase gene homologue (*stcA*) involved in bafilomycin production and
897 aerial mycelium formation in *Streptomyces* sp. SBI034. *Appl. Microbiol. Biotechnol.* 100:2749–
898 2760.
- 899 Jones, P., Garcia, B. J., Furches, A., Tuskan, G. A., and Jacobson, D. 2019. Plant host-associated
900 mechanisms for microbial selection. *Front. Plant Sci.* 10:862.

- 901 Kim, B.-Y., Zucchi, T. D., Fiedler, H.-P., and Goodfellow, M. 2012. *Streptomyces cocklensis* sp.
902 nov., a dioxamycin-producing actinomycete. *Int. J. Syst. Evol. Microbiol.* 62:279–283.
- 903 Kim, J.-N., Kim, Y., Jeong, Y., Roe, J.-H., Kim, B.-G., and Cho, B.-K. 2015. Comparative genomics
904 reveals the core and accessory genomes of *Streptomyces* species. *J. Microbiol. Biotechnol.*
905 25:1599–1605.
- 906 Konstantinidis, K. T., and Tiedje, J. M. 2005. Genomic insights that advance the species
907 definition for prokaryotes. *Proc. Natl. Acad. Sci. U. S. A.* 102:2567–2572.
- 908 Kuroha, T., Tokunaga, H., Kojima, M., Ueda, N., Ishida, T., Nagawa, S., et al. 2009. Functional
909 analyses of LONELY GUY cytokinin-activating enzymes reveal the importance of the direct
910 activation pathway in Arabidopsis. *Plant Cell.* 21:3152–3169.
- 911 Labeda, D. P., Dunlap, C. A., Rong, X., Huang, Y., Doroghazi, J. R., Ju, K.-S., et al. 2017.
912 Phylogenetic relationships in the family *Streptomycetaceae* using multi-locus sequence
913 analysis. *Antonie Van Leeuwenhoek.* 110:563–583.
- 914 Lamesch, P., Berardini, T. Z., Li, D., Swarbreck, D., Wilks, C., Sasidharan, R., et al. 2012. The
915 Arabidopsis Information Resource (TAIR): improved gene annotation and new tools. *Nucleic
916 Acids Res.* 40:D1202-1210.
- 917 Langmead, B., and Salzberg, S. L. 2012. Fast gapped-read alignment with Bowtie 2. *Nat.
918 Methods.* 9:357–359.
- 919 Levy, A., Salas Gonzalez, I., Mittelviehhaus, M., Clingenpeel, S., Herrera Paredes, S., Miao, J., et
920 al. 2017. Genomic features of bacterial adaptation to plants. *Nat. Genet.* 50:138–150.
- 921 Li, C., Jin, P., Liu, C., Ma, Z., Zhao, J., Li, J., et al. 2016. *Streptomyces bryophytorum* sp. nov., an
922 endophytic actinomycete isolated from moss (Bryophyta). *Antonie Van Leeuwenhoek.*
923 109:1209–1215.

- 924 Lichtenthaler, H. K., and Buschmann, C. 2001. Chlorophylls and carotenoids: measurement
925 and characterization by UV-VIS spectroscopy. *Curr. Protoc. Food Anal. Chem.* 1:F4.3.1-F4.3.8.
- 926 Love, M. I., Huber, W., and Anders, S. 2014. Moderated estimation of fold change and
927 dispersion for RNA-seq data with DESeq2. *Genome Biol.* 15:550.
- 928 Lundberg, D. S., Lebeis, S. L., Paredes, S. H., Yourstone, S., Gehring, J., Malfatti, S., et al. 2012.
929 Defining the core *Arabidopsis thaliana* root microbiome. *Nature.* 488:86–90.
- 930 Lynch, D., O’Brien, J., Welch, T., Clarke, P., Cuív, P. O., Crosa, J. H., et al. 2001. Genetic
931 organization of the region encoding regulation, biosynthesis, and transport of rhizobactin
932 1021, a siderophore produced by *Sinorhizobium meliloti*. *J. Bacteriol.* 183:2576–2585.
- 933 Ma, Q., Yang, Z., Pu, M., Peti, W., and Wood, T. K. 2011. Engineering a novel c-di-GMP-binding
934 protein for biofilm dispersal. *Environ. Microbiol.* 13:631–642.
- 935 Madhaiyan, M., Saravanan, V. S., See-Too, W.-S., Volpiano, C. G., Sant’Anna, F. H., Faria da
936 Mota, F., et al. 2022. Genomic and phylogenomic insights into the family *Streptomycetaceae*
937 lead to the proposal of six novel genera. *Int. J. Syst. Evol. Microbiol.* 72.
- 938 Martin, M. 2011. Cutadapt removes adapter sequences from high-throughput sequencing
939 reads. *EMBnet.journal.* 17:10–12.
- 940 McMurdie, P. J., and Holmes, S. 2013. phyloseq: an R package for reproducible interactive
941 analysis and graphics of microbiome census data. *PLoS One.* 8:e61217.
- 942 van der Meij, A., Worsley, S. F., Hutchings, M. I., and van Wezel, G. P. 2017. Chemical ecology
943 of antibiotic production by actinomycetes. *FEMS Microbiol. Rev.* 41:392–416.
- 944 Naseem, H., Ahsan, M., Shahid, M. A., and Khan, N. 2018. Exopolysaccharides producing
945 rhizobacteria and their role in plant growth and drought tolerance. *J. Basic Microbiol.*
946 58:1009–1022.

- 947 Olanrewaju, O. S., and Babalola, O. O. 2019. *Streptomyces*: implications and interactions in
948 plant growth promotion. *Appl. Microbiol. Biotechnol.* 103:1179–1188.
- 949 Ondov, B. D., Treangen, T. J., Melsted, P., Mallonee, A. B., Bergman, N. H., Koren, S., et al.
950 2016. Mash: fast genome and metagenome distance estimation using MinHash. *Genome Biol.*
951 17:132.
- 952 Parks, D. H., Imelfort, M., Skennerton, C. T., Hugenholtz, P., and Tyson, G. W. 2015. CheckM:
953 assessing the quality of microbial genomes recovered from isolates, single cells, and
954 metagenomes. *Genome Res.* 25:1043–1055.
- 955 Peng, L., Hocart, C. H., Redmond, J. W., and Williamson, R. E. 2000. Fractionation of
956 carbohydrates in *Arabidopsis* root cell walls shows that three radial swelling loci are
957 specifically involved in cellulose production. *Planta.* 211:406–414.
- 958 Perez-Riverol, Y., Bai, J., Bandla, C., García-Seisdedos, D., Hewapathirana, S., Kamatchinathan,
959 S., et al. 2022. The PRIDE database resources in 2022: a hub for mass spectrometry-based
960 proteomics evidences. *Nucleic Acids Res.* 50:D543–D552.
- 961 Pinski, A., Betekhtin, A., Hupert-Kocurek, K., Mur, L. A. J., and Hasterok, R. 2019. Defining the
962 genetic basis of Plant endophytic bacteria interactions. *Int. J. Mol. Sci.* 20.
- 963 Polkade, A. V., Mantri, S. S., Patwekar, U. J., and Jangid, K. 2016. Quorum sensing: an under-
964 explored phenomenon in the phylum Actinobacteria. *Front. Microbiol.* 7:131.
- 965 Poloni, A., and Schirawski, J. 2014. Red card for pathogens: phytoalexins in sorghum and
966 maize. *Mol. Basel Switz.* 19:9114–9133.
- 967 Prigent-Combaret, C., Prensier, G., Le Thi, T. T., Vidal, O., Lejeune, P., and Dorel, C. 2000.
968 Developmental pathway for biofilm formation in curli-producing *Escherichia coli* strains: role
969 of flagella, curli and colanic acid. *Environ. Microbiol.* 2:450–464.

- 970 Rizaludin, M. S., Stopnisek, N., Raaijmakers, J. M., and Garbeva, P. 2021. The chemistry of
971 stress: understanding the “cry for help” of plant roots. *Metabolites*. 11:357.
- 972 Rodríguez-Concepción, M., and Boronat, A. 2015. Breaking new ground in the regulation of
973 the early steps of plant isoprenoid biosynthesis. *Curr. Opin. Plant Biol.* 25:17–22.
- 974 Rohmer, M. 1999. The discovery of a mevalonate-independent pathway for isoprenoid
975 biosynthesis in bacteria, algae and higher plants. *Nat. Prod. Rep.* 16:565–574.
- 976 Salehi-Najafabadi, Z., Barreiro, C., Rodríguez-García, A., Cruz, A., López, G. E., and Martín, J. F.
977 2014. The gamma-butyrolactone receptors BulR1 and BulR2 of *Streptomyces tsukubaensis*:
978 tacrolimus (FK506) and butyrolactone synthetases production control. *Appl. Microbiol.*
979 *Biotechnol.* 98:4919–4936.
- 980 Schenk, S. T., and Schikora, A. 2015. AHL-priming functions via oxylipin and salicylic acid. *Front.*
981 *Plant Sci.* 5.
- 982 Schlaeppli, K., Dombrowski, N., Oter, R. G., Ver Loren van Themaat, E., and Schulze-Lefert, P.
983 2014. Quantitative divergence of the bacterial root microbiota in *Arabidopsis thaliana*
984 relatives. *Proc. Natl. Acad. Sci. U. S. A.* 111:585–592.
- 985 Schneider, J. C., Suzanne, H., and Somerville, C. R. 1995. Chilling-sensitive mutants of
986 *arabidopsis*. *Plant Mol. Biol. Report.* 13:11–17.
- 987 Seo, H., and Kim, K.-J. 2017. Structural basis for a novel type of cytokinin-activating protein.
988 *Sci. Rep.* 7:45985.
- 989 Shikura, N., Yamamura, J., and Nihira, T. 2002. *barS1*, a gene for biosynthesis of a gamma-
990 butyrolactone autoregulator, a microbial signaling molecule eliciting antibiotic production in
991 *Streptomyces* species. *J. Bacteriol.* 184:5151–5157.
- 992 Stassen, M. J. J., Hsu, S.-H., Pieterse, C. M. J., and Stringlis, I. A. 2021. Coumarin communication
993 along the microbiome–root–shoot axis. *Trends Plant Sci.* 26:169–183.

- 994 Świecimska, M., Golińska, P., and Goodfellow, M. 2022. Generation of a high quality library of
995 bioactive filamentous actinomycetes from extreme biomes using a culture-based
996 bioprospecting strategy. *Front. Microbiol.* 13:1054384.
- 997 Tittabutr, P., Awaya, J. D., Li, Q. X., and Borthakur, D. 2008. The cloned 1-aminocyclopropane-
998 1-carboxylate (ACC) deaminase gene from *Sinorhizobium* sp. strain BL3 in *Rhizobium* sp. strain
999 TAL1145 promotes nodulation and growth of *Leucaena leucocephala*. *Syst. Appl. Microbiol.*
1000 31:141–150.
- 1001 Uroz, S., Courty, P. E., and Oger, P. 2019. Plant symbionts are engineers of the plant-associated
1002 microbiome. *Trends Plant Sci.* 24:905–916.
- 1003 Vacheron, J., Desbrosses, G., Bouffaud, M.-L., Touraine, B., Moënne-Loccoz, Y., Muller, D., et
1004 al. 2013. Plant growth-promoting rhizobacteria and root system functioning. *Front. Plant Sci.*
1005 4:356.
- 1006 Vallenet, D., Belda, E., Calteau, A., Cruveiller, S., Engelen, S., Lajus, A., et al. 2013. MicroScope--
1007 an integrated microbial resource for the curation and comparative analysis of genomic and
1008 metabolic data. *Nucleic Acids Res.* 41:D636-647.
- 1009 Vallenet, D., Calteau, A., Cruveiller, S., Gachet, M., Lajus, A., Josso, A., et al. 2017. MicroScope
1010 in 2017: an expanding and evolving integrated resource for community expertise of microbial
1011 genomes. *Nucleic Acids Res.* 45:D517–D528.
- 1012 Vallenet, D., Engelen, S., Mornico, D., Cruveiller, S., Fleury, L., Lajus, A., et al. 2009.
1013 MicroScope: a platform for microbial genome annotation and comparative genomics.
1014 *Database J. Biol. Databases Curation.* 2009:bap021.
- 1015 Vallenet, D., Labarre, L., Rouy, Z., Barbe, V., Bocs, S., Cruveiller, S., et al. 2006. MaGe: a
1016 microbial genome annotation system supported by synteny results. *Nucleic Acids Res.* 34:53–
1017 65.

- 1018 Vannier, N., Agler, M., and Hacquard, S. 2019. Microbiota-mediated disease resistance in
1019 plants. *PLoS Pathog.* 15:e1007740.
- 1020 Vlot, A. C., Sales, J. H., Lenk, M., Bauer, K., Brambilla, A., Sommer, A., et al. 2021. Systemic
1021 propagation of immunity in plants. *New Phytol.* 229:1234–1250.
- 1022 Wang, Q., Liu, Q., Ma, Y., Zhou, L., and Zhang, Y. 2007. Isolation, sequencing and
1023 characterization of cluster genes involved in the biosynthesis and utilization of the
1024 siderophore of marine fish pathogen *Vibrio alginolyticus*. *Arch. Microbiol.* 188:433–439.
- 1025 Werner, T., Motyka, V., Laucou, V., Smets, R., Van Onckelen, H., and Schmölling, T. 2003.
1026 Cytokinin-deficient transgenic *Arabidopsis* plants show multiple developmental alterations
1027 indicating opposite functions of cytokinins in the regulation of shoot and root meristem
1028 activity. *Plant Cell.* 15:2532–2550.
- 1029 Wick, R. R., Judd, L. M., Gorrie, C. L., and Holt, K. E. 2017. Unicycler: Resolving bacterial genome
1030 assemblies from short and long sequencing reads. *PLoS Comput. Biol.* 13:e1005595.
- 1031 Wieczorek, S., Combes, F., Lazar, C., Giai Gianetto, Q., Gatto, L., Dorffer, A., et al. 2017. DAPAR
1032 & ProStaR: software to perform statistical analyses in quantitative discovery proteomics.
1033 *Bioinforma. Oxf. Engl.* 33:135–136.
- 1034 Woebbecke, D. M., Meyer, G. E., Von Bargen, K., and Mortensen, D. A. 1995. Color indices for
1035 weed identification under various soil, residue, and lighting conditions. *Trans. ASAE.* 38:259–
1036 269.
- 1037 Wood, D. E., Lu, J., and Langmead, B. 2019. Improved metagenomic analysis with Kraken 2.
1038 *Genome Biol.* 20:257.
- 1039 Wright, L. P., Rohwer, J. M., Ghirardo, A., Hammerbacher, A., Ortiz-Alcaide, M., Raguschke, B.,
1040 et al. 2014. Deoxyxylulose 5-phosphate synthase controls flux through the methylerythritol 4-
1041 phosphate pathway in *Arabidopsis*. *Plant Physiol.* 165:1488–1504.

- 1042 Xu, H., Luo, X., Qian, J., Pang, X., Song, J., Qian, G., et al. 2012. FastUniq: a fast de novo
1043 duplicates removal tool for paired short reads. PLOS ONE. 7:e52249.
- 1044 Zhang, L., Zhang, W., Li, Q., Cui, R., Wang, Z., Wang, Y., et al. 2020. Deciphering the root
1045 endosphere microbiome of the desert plant *Alhagi sparsifolia* for drought resistance-
1046 promoting bacteria. Appl. Environ. Microbiol. 86:e02863-19.
- 1047

1048 **LEGENDS TO FIGURES**

1049 **Figure 1. Schematic representation of the major metabolic capacities in *A. bryophytorum* DSM 42138 or *S. cocklensis* DSM 42063.** These
1050 capacities were ascertained using genomic data. Blue, Plant-bacteria interaction capacities of *S. cocklensis* DSM 42063; Green, Plant-bacteria
1051 interaction capacities of *A. bryophytorum* DSM 42138; Red, Carbon and phosphate metabolism capacities of both bacteria. Created with
1052 BioRender.com.

1053 **Figure 2. Electronic microscopy of seeds and leaves of wild-type (WT) or *chs5* mutant *A. thaliana* inoculated with *A. bryophytorum* DSM
1054 42138 or *S. cocklensis* DSM 42063.** (A) Bacteria observed on the seed surface 4 days after inoculation. (B) Leaves of wild-type seedlings
1055 inoculated with *S. cocklensis* DSM 42063. Pictures were taken 24 days after inoculation. Bacteria are indicated by an arrow. NI: Non-inoculated.
1056 +42063: inoculated with *S. cocklensis* DSM 42063. +42138: inoculated with *A. bryophytorum* DSM 42138.

1057 **Figure 3. Normalized abundance of the OTUs identified as *A. bryophytorum* DSM 42138 or *S. cocklensis* DSM 42063.**

1058 *p*-values (ANOVA) were calculated for the two major OTUs, cluster-2 and cluster-3 corresponding to *A. bryophytorum* DSM 42138 or *S. cocklensis*
1059 DSM 42063. *: *p*-values < 0,05; **: *p*-values < 0,01.

1060 **Figure 4. Growth of wild-type (WT) or *chs5* mutant seedlings inoculated with *A. bryophytorum* DSM 42138 or *S. cocklensis* DSM 42063.**

1061 Total seedling surface was measured using Image J, 24 (left) and 31 (right) days after inoculation- NI: Non-inoculated. The statistical relevance
1062 was analyzed using a non-parametric Kruskal-Wallis test and the *p*-value were evaluated with a Dunn test and the Bonferroni correction. (A: $X^2(5)$
1063 = 40.15, *p*-value ≤ 0.0001 , n = 478; (b): $X^2(5) = 216.36$, *p*-value ≤ 0.0001 , n = 478). ***: *p*-value $\leq 10^{-4}$; **** *p*-value $\leq 10^{-5}$.

1064 **Figure 5. Effect of bacterial inoculations on the *Arabidopsis thaliana* proteome.** The Benjamini p -value ($-\log_{10}$) (y-axis) calculated for each
1065 GO term was plotted against the number of *A. thaliana* differentially expressed proteins related to one GO term (x-axis). The GO terms were
1066 arranged in three categories (molecular functions in red, biological processes in green and cellular components in blue). The bubbles size illustrates
1067 the fold enrichment for each GO term. NI: Non-inoculated. +42063: inoculated with *S. cocklensis* DSM 42063. +42138: inoculated with *A.*
1068 *bryophytorum* DSM 42138.

1069

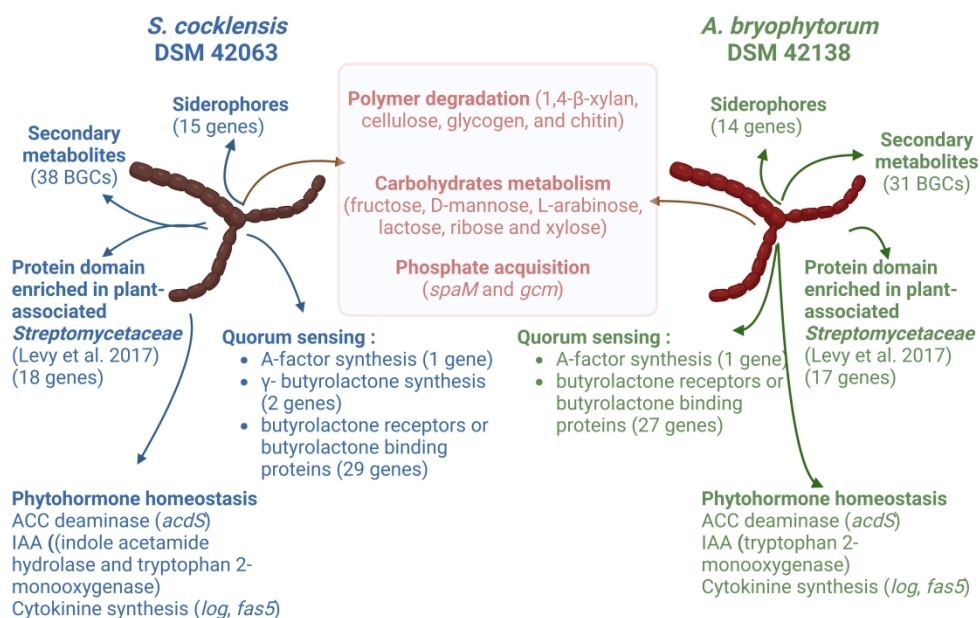


Figure 1. Schematic representation of the major metabolic capacities in *A. bryophytorum* DSM 42138 or *S. cocklensis* DSM 42063. These capacities were ascertained using genomic data. Blue, Plant-bacteria interaction capacities of *S. cocklensis* DSM 42063; Green, Plant-bacteria interaction capacities of *A. bryophytorum* DSM 42138; Red, Carbon and phosphate metabolism capacities of both bacteria. Created with BioRender.com.

254x177mm (600 x 600 DPI)

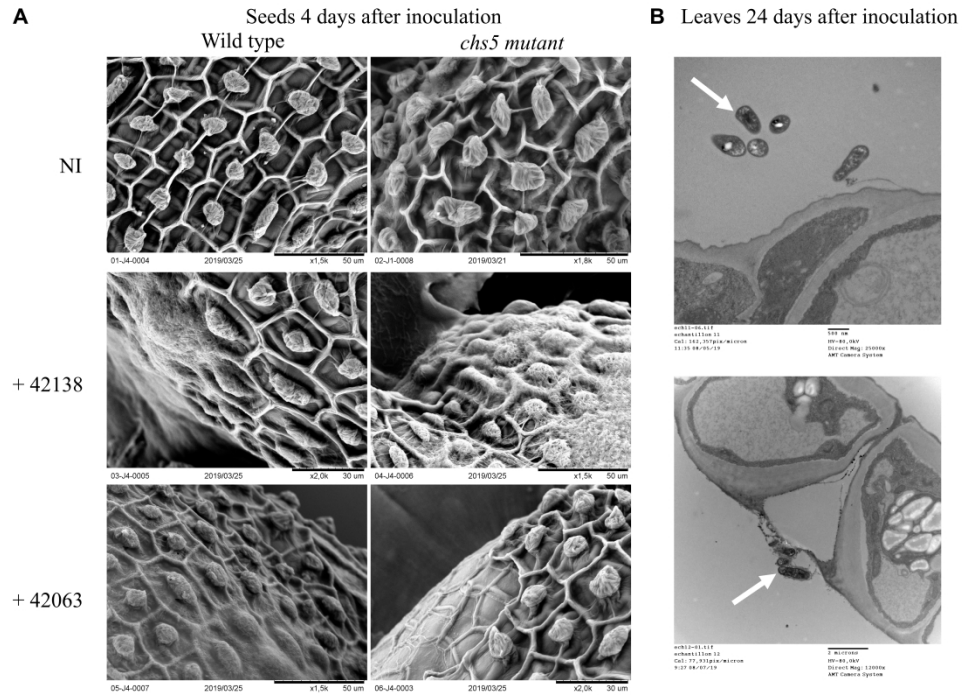


Figure 2. Electronic microscopy of seeds and leaves of wild-type (WT) or *chs5* mutant *A. thaliana* inoculated with *A. bryophytorum* DSM 42138 or *S. cocklensis* DSM 42063. (A) Bacteria observed on the seed surface 4 days after inoculation. (B) Leaves of wild-type seedlings inoculated with *S. cocklensis* DSM 42063. Pictures were taken 24 days after inoculation. Bacteria are indicated by an arrow. NI: Non-inoculated. +42063: inoculated with *S. cocklensis* DSM 42063. +42138: inoculated with *A. bryophytorum* DSM 42138.

1237x875mm (144 x 144 DPI)

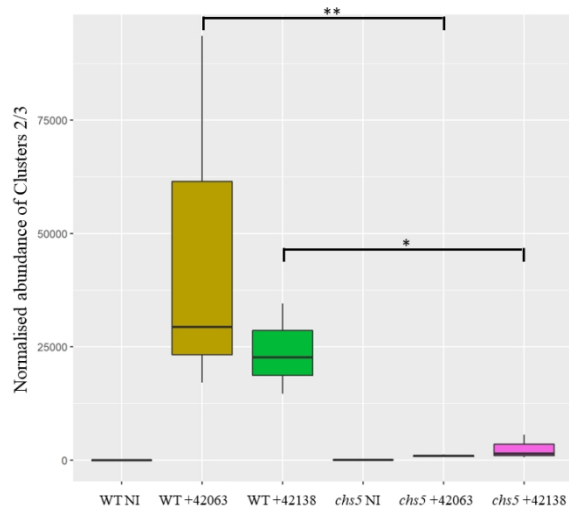


Figure 3. Normalized abundance of the OTUs identified as *A. bryophytorum* DSM 42138 or *S. cocklensis* DSM 42063. p-values (ANOVA) were calculated for the two major OTUs, cluster-2 and cluster-3 corresponding to *A. bryophytorum* DSM 42138 or *S. cocklensis* DSM 42063. *: p-values < 0,05; **: p-values < 0,01.

338x190mm (96 x 96 DPI)

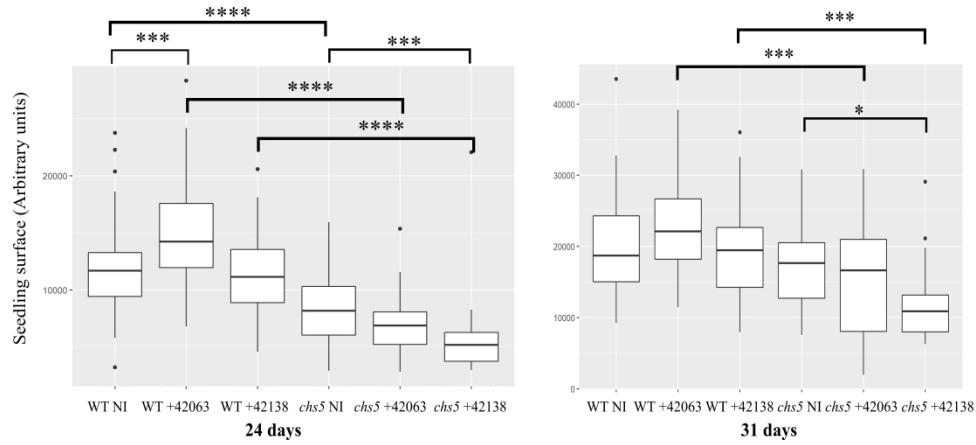


Figure 4. Growth of wild-type (WT) or *chs5* mutant seedlings inoculated with *A. bryophytorum* DSM 42138 or *S. cocklensis* DSM 42063. Total seedling surface was measured using Image J, 24 (left) and 31 (right) days after inoculation- NI: Non-inoculated. The statistical relevance was analyzed using a non-parametric Kruskal-Wallis test and the p-value were evaluated with a Dunn test and the Bonferroni correction. (A: $X^2(5) = 40.15$, p-value ≤ 0.0001 , n = 478; (b): $X^2(5) = 216.36$, p-value ≤ 0.0001 , n = 478). ***: p-value $\leq 10^{-4}$; ****: p-value $\leq 10^{-5}$.

1228x531mm (144 x 144 DPI)

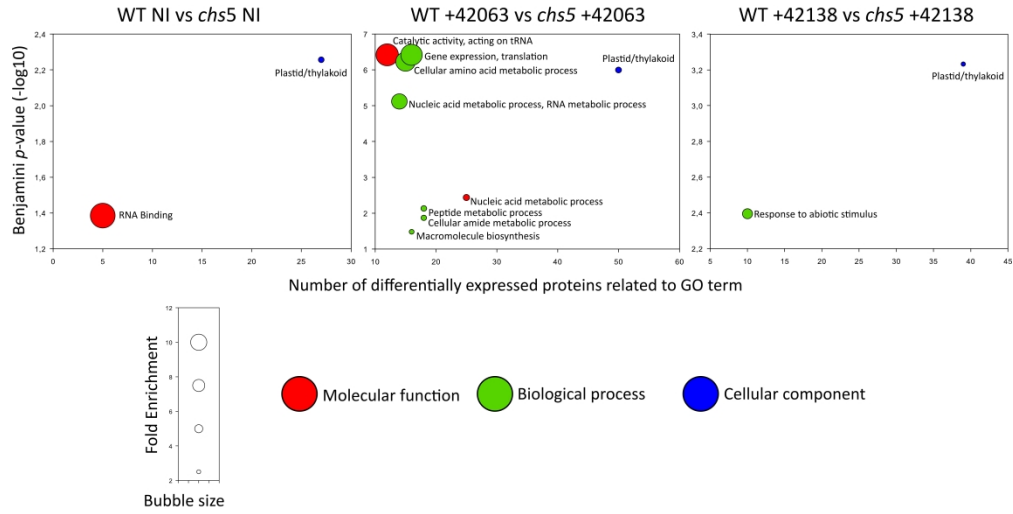


Figure 5. Effect of bacterial inoculations on the *Arabidopsis thaliana* proteome. The Benjamini p-value ($-\log_{10}$) (y-axis) calculated for each GO term was plotted against the number of *A. thaliana* differentially expressed proteins related to one GO term (x-axis). The GO terms were arranged in three categories (molecular functions in red, biological processes in green and cellular components in blue). The bubbles size illustrates the fold enrichment for each GO term. NI: Non-inoculated. +42063: inoculated with *S. cockleensis* DSM 42063. +42138: inoculated with *A. bryophytorum* DSM 42138.

1182x620mm (144 x 144 DPI)

1 SUPPLEMENTARY MATERIAL

2

3 **Figure S1: Mash-based Phylogram generated with 187 *Streptomycetaceae* whole genomes.**

4 Mash distances are computed with kmer size = 18 and sketch size = 5000. Colors group the
5 different species. Contaminated or incomplete genomes (not associated to MICGC clusters) are
6 displayed in black. The pairwise genome distance were calculated using Mash, which strongly
7 correlates with the Average Nucleotide Identity (ANI) (Ondov et al. 2016; Konstantinidis and
8 Tiedje 2005).

9 **Figure S2. Pan-, Variable- and Core-genome of *A. bryophytorum* DSM 42138 or *S.***

10 *cocklensis* DSM 42063. The Venn diagram shows the specific or shared families of genes.

11 **Figure S3. Observations of wild-type (WT) or *chs5* mutant seedlings inoculated with *A.***

12 *bryophytorum* DSM 42138 or *S. cocklensis* DSM 42063. The Seedlings have been
13 photographed 24 days after inoculation.

14 **Figure S4. Additional pictures for electronic microscopy of seeds and leaves of wild-type**

15 **(WT) or *chs5* mutant *A. thaliana* inoculated with *A. bryophytorum* DSM 42138 or *S.***

16 *cocklensis* DSM 42063. (A) Bacteria observed on the seed surface 0 (D0), 1 (D1) or 4 (D4)

17 days after inoculation. (B) Electronic microscopy of leaves from wild-type seedlings inoculated

18 with *S. cocklensis* DSM 42063. Pictures were taken 24 days after inoculation. Bacteria are

19 indicated by an arrow. NI: Non-inoculated. +42063: inoculated with *S. cocklensis* DSM 42063.

20 +42138: inoculated with *A. bryophytorum* DSM 42138.

21 **Figure S5. Comparison of the abundance (%) of the different phyla, identified in the wild**

22 **type (WT) or *chs5* mutant seedlings during *in vitro* studies. (A) The relative abundance of**

23 each phylum in the total microbiota is expressed after down-sampling. (B) Total normalized

24 abundance of the OTUs identified. *p*-values are indicated for the two major OTUs, cluster-2

25 and cluster-3. No: no bacterium. mut = *chs5*. Sbrv = inoculated with *A. bryophytorum*. Scoc =
26 inoculated with *S. cocklensis*.

27 **Figure S6: Green intensity and chlorophylls contents of wild-type (WT) or *chs5* seedlings**

28 **inoculated with *A. bryophytorum* DSM 42138 or *S. cocklensis* DSM 42063.** (A) The green

29 intensity of seedlings was measured using Image J, after 24 days of inoculation. The statistical

30 relevance was analyzed using a non-parametric Kruskal-Wallis test and the *p*-values were

31 evaluated with a Dunn test and the Bonferroni correction. (A: $X^2(5) = 130.87$, $p\text{-value} \leq 0.0001$,

32 $n = 478$. *: $p\text{-value} \leq 10^{-3}$; **** $p\text{-value} \leq 10^{-6}$). (B) Chlorophyll a and b, xanthophylls and

33 carotenoids content was shown for 15 plants. (C) Chlorophyll a and b, xanthophylls and

34 carotenoids quantities were expressed per mg dry weight. c_a : concentration of chlorophyll a; c_b :

35 concentration of chlorophyll b; $c_{(x+c)}$: concentration of xanthophylls and carotenes. The

36 normality and equality of variances were verified with a Shapiro-Wilk test and a Bartlett test,

37 respectively, and a statistical one-way ANOVA test was performed. NS: non-significant. NI:

38 Non-inoculated. +42063: inoculated with *S. cocklensis* DSM 42063. +42138: inoculated with

39 *A. bryophytorum* DSM 42138.

40 **Figure S7: Correlation curve between surface and green intensity of plants grown *in vitro*.**

41 Pearson's product-moment correlation was calculated. *p*-values are presented on each graph.

42 Significant correlation was assigned when $p\text{-value} < 0.01$. WT: wild type. NI: Non-inoculated.

43 + DSM 42063: inoculated with *S. cocklensis* DSM 42063. +DSM 42138: inoculated with *A.*

44 *bryophytorum* DSM 42138.

45 SUPPLEMENTARY TABLES

46 **Table S1: Primers used for 16S RNA encoding gene amplification**

Name of Sequences the primer		reference
799F		(Bulgarelli et al. 2013; Schlaeppli et al. 2014)
799F1	5'-TCGTCGGCAGCGTCAGATGTGTATAAGAGACAGAACMGGATTAGATACCCCKG-3'	(Graindorge et al. 2022)
799F2	5'-TCGTCGGCAGCGTCAGATGTGTATAAGAGACAGTAACMGGATTAGATACCCCKG-3'	(Graindorge et al. 2022)
799F3	5'-TCGTCGGCAGCGTCAGATGTGTATAAGAGACAGGTAACMGGATTAGATACCCCKG-3'	(Graindorge et al. 2022)
799F4	5'-TCGTCGGCAGCGTCAGATGTGTATAAGAGACAGCGAAACMGGATTAGATACCCCKG-3'	(Graindorge et al. 2022)
799F5	5' –TCGTCGGCAGCGTCAGATGTGTATAAGAGACAGATGAAACMGGATTAGATACCCCKG- 3'	(Graindorge et al. 2022)
799F6	5'-TCGTCGGCAGCGTCAGATGTGTATAAGAGACAGTGCGAAACMGGATTAGATACCCCKG- 3'	(Graindorge et al. 2022)
799F7	5' –TCGTCGGCAGCGTCAGATGTGTATAAGAGACAGGAGTGGAACMGGATTAGATACCCCKG- 3'	(Graindorge et al. 2022)
1193R	5' –TCGTCGGCAGCGTCAGATGTGTATAAGAGACAGCTTGTGGAACMGGATTAGATACCCCKG- 3'	(Graindorge et al. 2022)
1193R1	5'-GTCTCGTGGGCTCGGAGATGTGTATAAGAGACAGACGTCATCCCCACCTTCC-3'	(Bulgarelli et al. 2013; Schlaeppli et al. 2014)
1193R2	5'-GTCTCGTGGGCTCGGAGATGTGTATAAGAGACAGTACGTCATCCCCACCTTCC-3'	(Graindorge et al. 2022)
1193R3	5'-GTCTCGTGGGCTCGGAGATGTGTATAAGAGACAGGTACGTCATCCCCACCTTCC-3'	(Graindorge et al. 2022)

1193R4	5'-GTCTCGTGGGCTCGGAGATGTGTATAAGAGACAGCGAACGTCATCCCCACCTTCC-3'	(Graindorge et al. 2022)
1193R5	5' -GTCTCGTGGGCTCGGAGATGTGTATAAGAGACAGATGAACGTCATCCCCACCTTCC- 3'	(Graindorge et al. 2022)
1193R6	5' –GTCTCGTGGGCTCGGAGATGTGTATAAGAGACAGTGCGAACGTCATCCCCACCTTCC- 3'	(Graindorge et al. 2022)
1193R7	5' –GTCTCGTGGGCTCGGAGATGTGTATAAGAGACAGGAGTGGACGTCATCCCCACCTTCC- 3'	(Graindorge et al. 2022)
	5' –GTCTCGTGGGCTCGGAGATGTGTATAAGAGACAGCTTGTGGACGTCATCCCCACCTTCC- 3'	(Graindorge et al. 2022)

48 **Table S2. General characteristics of the *S. cocklensis* DSM 42063 and *A. bryophytorum***
 49 **DSM 42138 genomes.**

Genome characteristics	DSM42063	DSM42138
Size (bp)	9153011	8071242
GC-content (%)	72.05	72.50
Predicted CDS	9117	8046
Genome coding (%)	88.44	90.27
Average CDS size (bp)	940.3	979.03
Number of tRNA	20	20
Number of 16S encoding gene	1	1
ORF of unknown function (%)	3232 (35.45)	2707 (33.67)
Repetitive regions (%) ^a	9.37	8.44
Nb of scaffold	135	23
Completeness (%) ^b	99.47	99.47
Putative genes involved in plant-bacteria interactions		
Polymer degradation	1,4- β -xylan, cellulose, glycogen, and chitin	1,4- β -xylan, cellulose, glycogen, and chitin
Genes involved in metabolism of	fructose, D-mannose, L-arabinose, lactose, ribose and xylose	fructose, D-mannose, L-arabinose, lactose, ribose and xylose
Nitrogen fixation	nd ^c	nd ^c
Siderophore	SCOCK_v1_190099-SCOCK_v1_190102, SCOCK_v1_310026 (<i>rhbACDF</i>), SCOCK_v1_500009-SCOCK_v1_500011 and SCOCK_v1_220108-SCOCK_v1_220110 (<i>feuV-fepDG, gobMP</i>), SCOCK_v1_100083-SCOCK_v1_100086 ^d (<i>pvsABCDE</i>)	SBRY_v2_60544-SBRY_v2_60547, SBRY_v2_20954 (<i>rhbACDF</i>), SBRY_v2_30340-SBRY_v2_30344 and SBRY_v2_40121-SBRY_v2_40124 (<i>feuV-fepDG, gobMP</i>)
Phosphate acquisition	SCOCK_v1_20358 (<i>gpm</i>) SCOCK_v1_210117 SCOCK_v1_320067 (<i>sapM</i>) SCOCK_v1_430054 (<i>gpm</i>)	SBRY_v2_20102 (<i>gpm</i>) SBRY_v2_20729 (<i>sapM</i>) SBRY_v2_40074 SBRY_v2_140108 (<i>gpm</i>)
<i>Quorum sensing</i>		
A-factor synthesis (γ -butyrolactone)	SCOCK_v1_30036 (<i>barS</i>) ^d , SCOCK_v1_60217 and SCOCK_v1_70112 ^d	SBRY_v2_50115

Number of genes encoding putative butyrolactone receptors or butyrolactone binding proteins	29	27
<i>Phytohormone homeostasis</i>		
ACC-deaminase	SCOCK_v1_360062 (<i>acdS</i>)	SBRY_v2_10788 (<i>acdS</i>)
IAA synthesis	SCOCK_v1_140087 (indole acetamide hydrolase) ^d and SCOCK_v1_270097 (tryptophan 2-monooxygenase)	SBRY_v2_70106 (tryptophan 2-monooxygenase),
Cytokinin synthesis	SCOCK_v1_390035, SCOCK_v1_130169 (<i>log</i>)	SBRY_v2_10668, SBRY_v2_11141 (<i>log</i>), SBRY_v2_100168 (<i>fas5</i>) ^d
<i>Secondary metabolites</i>		
Number of BGCs (AntiSMASH)	37	30
	carotenoids (isorenieratene), antibiotics or antifungal compounds (griseusins, Curamycin), bioactive molecules (alkylresorcinol, pristinol, 1-heptadecene, ketomemicin), VOCs (geosmin, 2-methylisoborneol)	carotenoids (isorenieratene), antibiotics or antifungal compounds (griseusins, Curamycin), antibacterial lipopeptide rhizomide, bioactive molecules (alkylresorcinol, pristinol, 1-heptadecene), VOCs (geosmin, 2-methylisoborneol)
<i>Biofilm formation and regulation</i>		
Number of genes involved in colanic acid synthesis	21 genes (SCOCK_v1_280106 ^d) SCOCK_v1_190032 (<i>vbfa</i>), SCOCK_v1_100057 and SCOCK_v1_250124 (<i>bdcA</i>)	18 genes SBRY_v2_60465 (<i>vbfa</i>), SBRY_v2_11100 (<i>bdcA</i>)
<i>Protein domain enriched in plant-associated Streptomycetaceae^e</i>		
Pfam00295 (Glycosyl hydrolases family 28)	SCOCK_v1_150111 ^d	SBRY_v2_100229 ^d
Pfam02705 (putative potassium transport system protein kup)	SCOCK_v1_60101 ^d	SBRY_v2_50187 ^d
Pfam03239 (iron transporter FTR1 family)	SCOCK_v1_140217, SCOCK_v1_20006	SBRY_v2_20515, SBRY_v2_40652
Pfam16355 (Beta-galactosidase)	SCOCK_v1_60045	SBRY_v2_50249

Pfam00190 (Cupin)	SCOCK_v1_70084	SBRY_v2_30541
Pfam00544 (Pectate lyase)	SCOCK_v1_590017, SCOCK_v1_80248	SBRY_v2_40509, SBRY_v2_40889
Pfam01095 (Pectinesterase)	SCOCK_v1_380033, SCOCK_v1_400051	SBRY_v2_120034, SBRY_v2_40833
Pfam01179 (Copper amine oxidase, enzyme domain)	SCOCK_v1_140167 ^d , SCOCK_v1_170004	SBRY_v2_70400
Pfam01301 (Glycosyl hydrolases family 35)	SCOCK_v1_110049, SCOCK_v1_170044, SCOCK_v1_280088, SCOCK_v1_770022	SBRY_v2_130007, SBRY_v2_40253, SBRY_v2_40751, SBRY_v2_80165
Pfam02727 (Copper amine oxidase, N2 domain)	SCOCK_v1_170004	SBRY_v2_70400
Pfam02728 (Copper amine oxidase, N3 domain)	SCOCK_v1_170004	SBRY_v2_70400

50 ^aCalculation of repetitive regions did not include undetermined ('N') bases. ^bCompleteness
51 was estimated using CheckM (Parks et al. 2015). ^cnd : Not found. ^dStrain-specific genes.
52 ^ePfam domains reproducibly enriched in plant-associated *Streptomyetaceae* genomes
53 predicted with five independent statistical approach by (Levy et al. 2017), or plant-resembling
54 plant-associated and root-associated domains (PREPARADOs) enriched in plant associated
55 *Streptomyetaceae* and highlighted by (Levy et al. 2017).
56

Table S3. Bacterial proteins identified in plants inoculated with *A. bryophytorum* or *S. cocklensis*

Accession	Found in plants/inoculated with	Description	Function
Bacterial proteins identified with <i>A. bryophytorum</i> or <i>S. cocklensis</i> specific peptides (7 proteins)			
SBRY_v2_100019 ID:85706936	Col-0 / <i>A. bryophytorum</i>	ABC transporter substrate-binding protein	[G] Carbohydrate transport and metabolism
SCOCK42063_v1_650034 ID:72902332 ahcY	Col-0 / <i>S. cocklensis</i>	Adenosylhomocysteinase	[H] Coenzyme transport and metabolism,
SCOCK42063_v1_70039 ID:72896013	Col-0 / <i>S. cocklensis</i>	Arylsulfotransferase (ASST)	[S] Function unknown
SBRY_v2_10287 ID:85700244 groEL	Col-0 / <i>A. bryophytorum</i>	Chaperonin large subunit	[O] Post-translational modification, protein turnover, and chaperones
SBRY_v2_10186 ID:85700143 rpsG	Col-0 / <i>A. bryophytorum</i>	Ribosomal protein S7	[J] Translation, ribosomal structure and biogenesis
SCOCK42063_v1_120081 ID:72897190 rp1A	Col-0 / <i>S. cocklensis</i>	Ribosomal protein L1	[J] Translation, ribosomal structure and biogenesis
SBRY_v2_60368 ID:85705648	Col-0 / <i>A. bryophytorum</i>	D-xylose transport system substrate-binding protein	[G] Carbohydrate transport and metabolism
Bacterial proteins identified with peptides matching with both <i>A. bryophytorum</i> and <i>S. cocklensis</i> proteomes (16 proteins)			
SCOCK42063_v1_200106 ID:72898820 rpsF or SBRY_v2_50631 ID:85705042 rpsF or 15 other trembl accession	Col-0 / <i>S. cocklensis</i>	30S ribosomal protein S6	[J] Translation, ribosomal structure and biogenesis
SBRY_v2_30377 ID:85702840 groEL or SCOCK42063_v1_220073 ID:72899145 groEL or 340 other trembl accession	Col-0 / <i>S. cocklensis</i> ; Col-0 / <i>A. bryophytorum</i>	Chaperonin large subunit	[O] Post-translational modification, protein turnover, and chaperones

SBRY_v2_10077 ID:85700034 cspC or SCOCK42063_v1_710030 ID:72902524 cspC or 6 other trembl accession	Col-0 / <i>S. cocklensis</i> ; Col-0 / <i>A. bryophytorum</i>	Cold-shock protein	[K] Transcription
SBRY_v2_11162 ID:85701119 serA or SCOCK42063_v1_130144 ID:72897479 serA SBRY_v2_30075 ID:85702538 eno or SCOCK42063_v1_90166 ID:72896669 eno or tr A0A1M7F5J0 A0A1M7F5J0_9ACTN	Col-0 / <i>A. bryophytorum</i> Col-0 / <i>S. cocklensis</i> ; Col-0 / <i>A. bryophytorum</i>	D-3-phosphoglycerate dehydrogenase Enolase	[E] Amino acid transport and metabolism [G] Carbohydrate transport and metabolism
SBRY_v2_110199 ID:85707376 or tr A0A1M7PAY2 A0A1M7PAY2_9ACTN	Col-0 / <i>A. bryophytorum</i>	Putative thiosulfate sulfurtransferase	[P] Inorganic ion transport and metabolism
SBRY_v2_30380 ID:85702843 or SCOCK42063_v1_220068 ID:72899140 or 764 other trembl accession	Col-0 / <i>A. bryophytorum</i>	Threonine synthase	[E] Amino acid transport and metabolism
SBRY_v2_40138 ID:85703601 or tr A0A0M8VEZ0 A0A0M8VEZ0_9ACTN or tr A0A560XHT1 A0A560XHT1_9ACTN or tr A0A5P1YKK5 A0A5P1YKK5_STRTE	Col-0 / <i>A. bryophytorum</i>	Predicted oxidoreductase	[C] Energy production and conversion
SCOCK42063_v1_130048 ID:72897383 rpsB or SBRY_v2_11262 ID:85701219 rpsB or 587 other trembl accession	Col-0 / <i>S. cocklensis</i>	30S ribosomal protein S2	[J] Translation, ribosomal structure and biogenesis
SBRY_v2_11343 ID:85701300 rpsO or SCOCK42063_v1_510009 ID:72901676 rpsO or 243 other trembl accession	Col-0 / <i>S. cocklensis</i>	Ribosomal protein S15	[J] Translation, ribosomal structure and biogenesis
SBRY_v2_60368 ID:85705648 or SCOCK42063_v1_600017 ID:72902098 or tr A0A1M7LJ96 A0A1M7LJ96_9ACTN	Col-0 / <i>S. cocklensis</i> ; Col-0 / <i>A. bryophytorum</i> ; Chs-5 / <i>A. bryophytorum</i>	D-xylose transport system substrate-binding protein	[G] Carbohydrate transport and metabolism

SBRY_v2_20998 ID:85702307 gapA or 6 other trembl accession	Col-0 / <i>A. bryophytorum</i>	Glyceraldehyde-3-phosphate dehydrogenase (NAD- dependent, glycolytic)	[G] Carbohydrate transport and metabolism
SBRY_v2_10241 ID:85700198 rplE or SCOCK42063_v1_120131 ID:72897240 rplE or 119 other trembl accession	Col-0 / <i>A. bryophytorum</i>	Ribosomal protein L5	[J] Translation, ribosomal structure and biogenesis
SCOCK42063_v1_120136 ID:72897245 rpsE or SBRY_v2_10246 ID:85700203 rpsE or 6 other trembl accession	Col-0 / <i>S. cocklensis</i>	30S ribosomal protein S5	[J] Translation, ribosomal structure and biogenesis
SCOCK42063_v1_230015 ID:72899241 gapA or tr A0A1M7DMT1 A0A1M7DMT1_9ACTN	Col-0 / <i>S. cocklensis</i>	Glyceraldehyde-3-phosphate dehydrogenase (NAD- dependent, glycolytic)	[G] Carbohydrate transport and metabolism
SCOCK42063_v1_520034 ID:72901741 or tr A0A1H0KDK6 A0A1H0KDK6_9ACTN or tr A0A4U0SP23 A0A4U0SP23_9ACTN	Col-0 / <i>S. cocklensis</i>	NitT/TauT family transport system substrate-binding protein	[P] Inorganic ion transport and metabolism

59 **Table S4: *A. thaliana* proteins differentially abundant in the wild type as compared to *chs5*, and/or in inoculated or non-inoculated plants**

60 **cultivated *in vitro*.** NS: Non-Significant. LogFC: Log2Fold Change

61

Figure S1

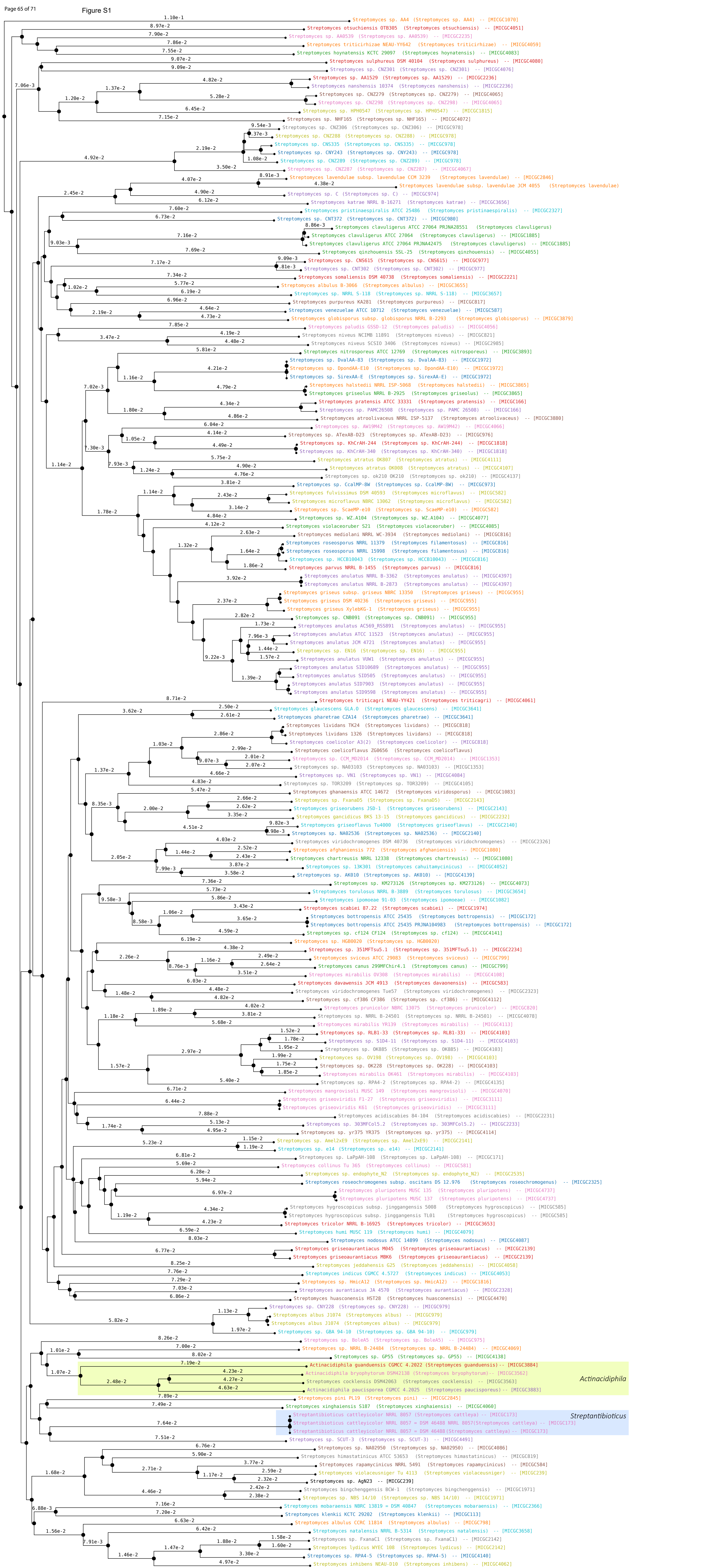


Figure S2

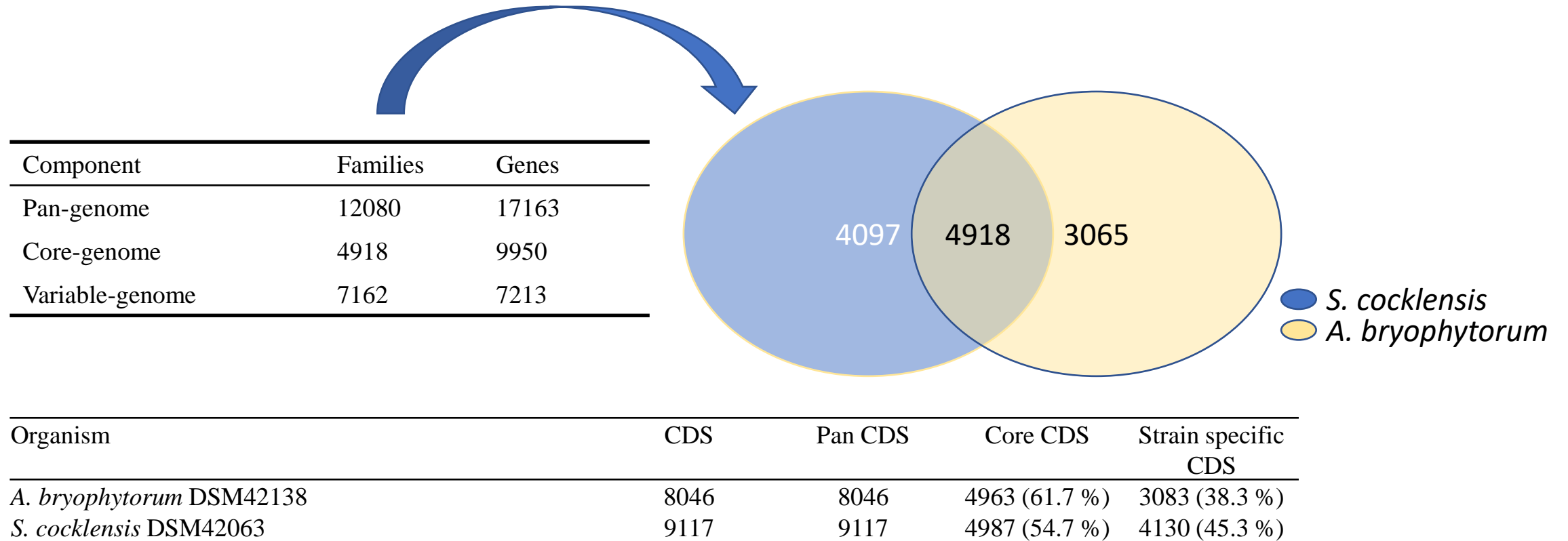
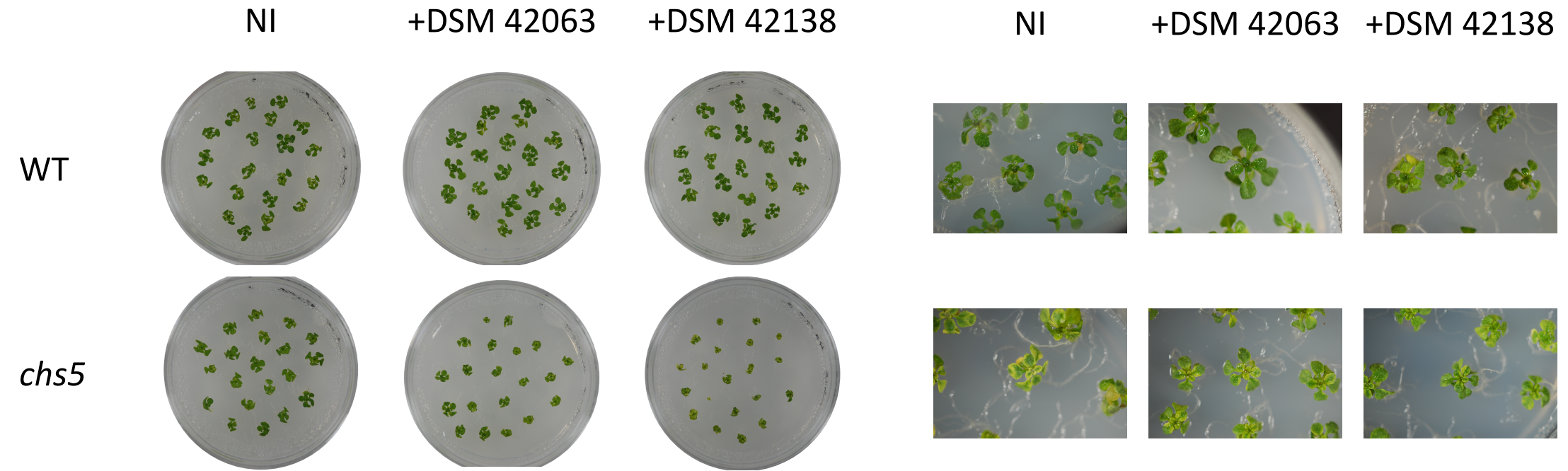


Figure S3



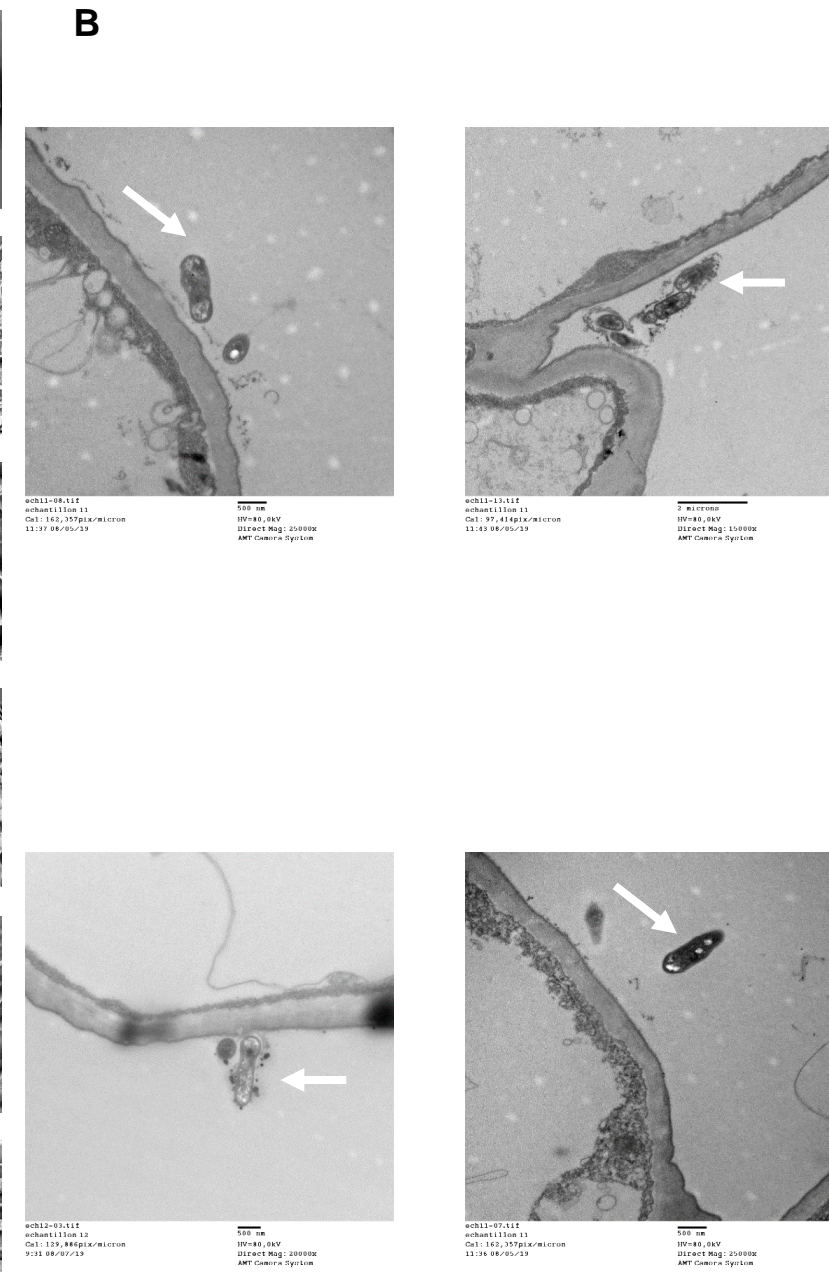
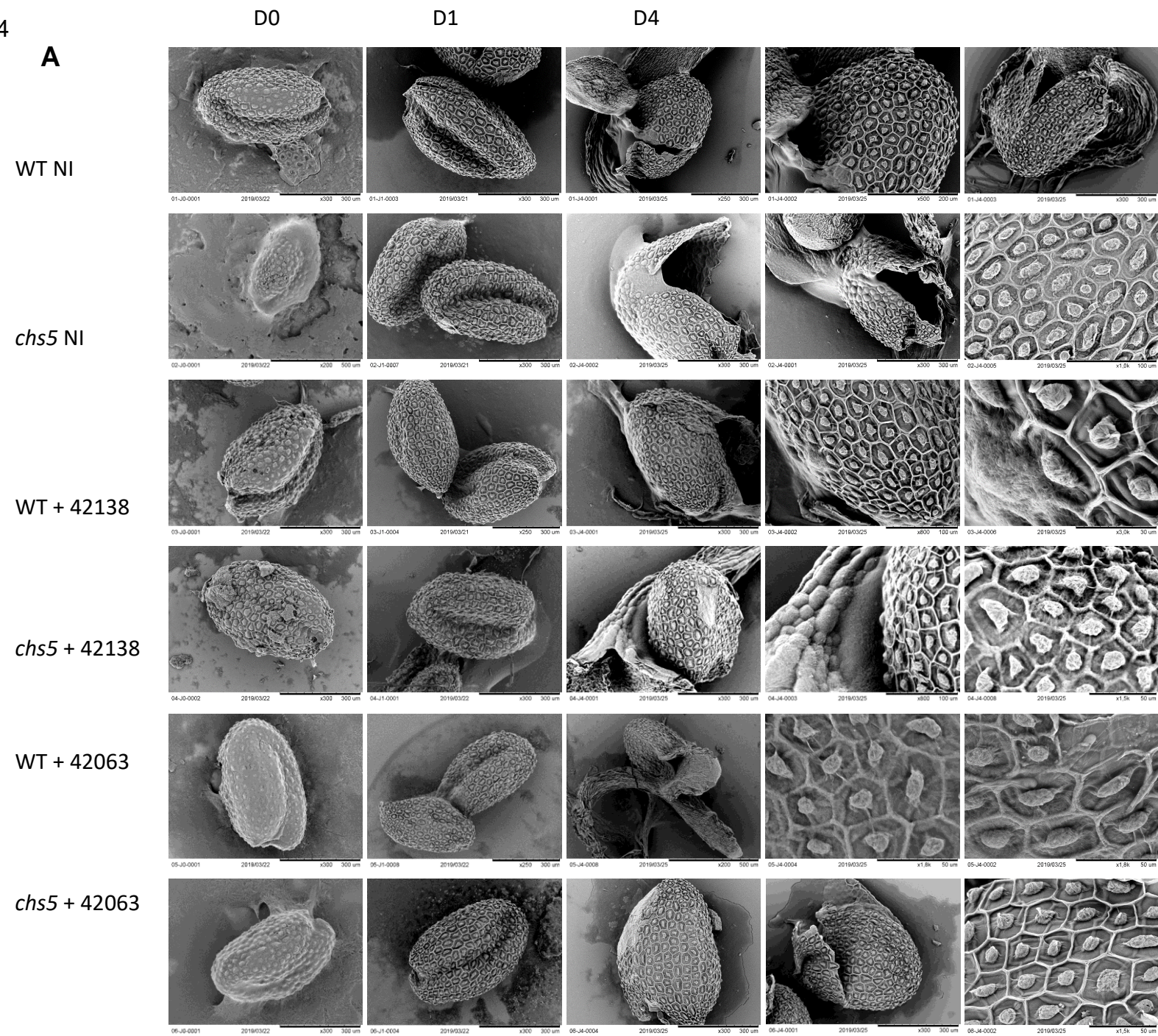
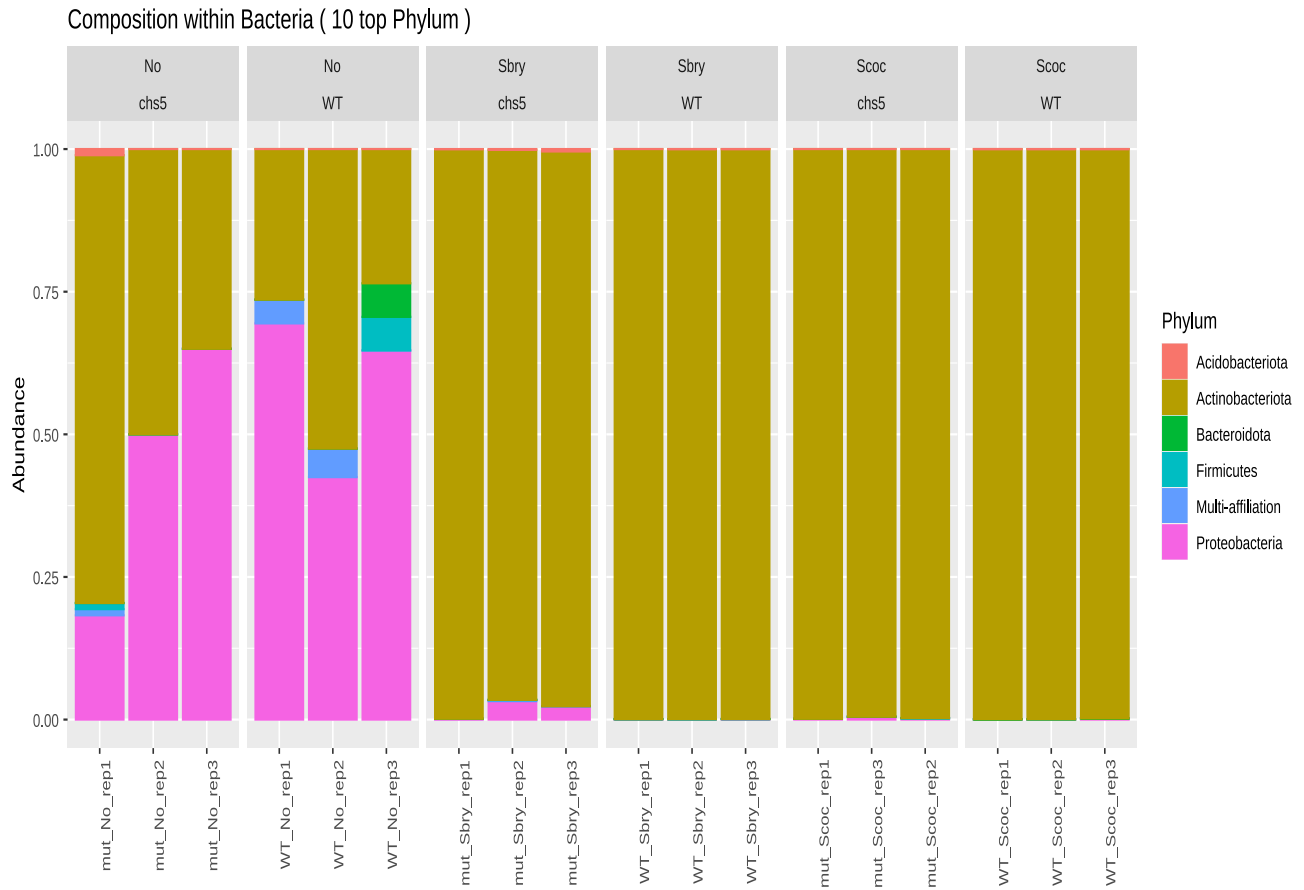


Figure S5

A Relative abundance after down-sampling



B

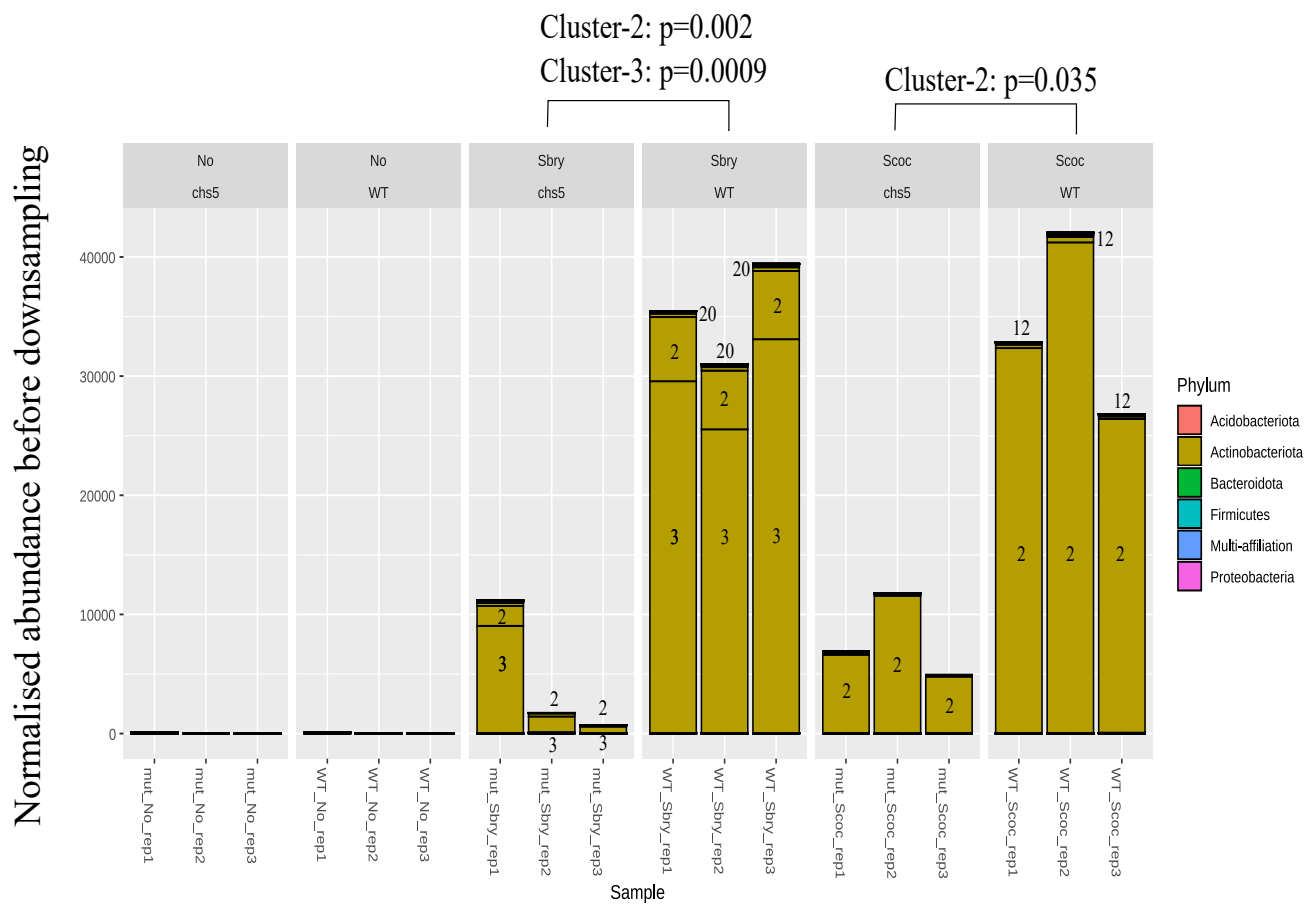


Figure S7

